PHILOSOPHICAL TRANSACTIONS OF THE ROYAL SOCIETY A MATHEMATICAL, PHYSICAL & ENGINEERING SCIENCES

The Initiation of Detonation from General Non-Uniformly Distributed Initial Conditions

Mark Short

Phil. Trans. R. Soc. Lond. A 1995 **353**, 173-203
doi: 10.1098/rsta.1995.0097

The initiation of detonation from general non-uniformly distributed initial conditions

By Mark Short

School of Mathematics, University of Bristol, Bristol BS8 1TW, UK

The chemical evolution of a hot gas subject to initial non-uniformities in velocity, pressure, temperature and reactant mass concentration is studied for moderate activation energies. It is demonstrated that such initial non-uniformities generate gradients in the distribution of chemical ignition times for each fluid particle, resulting in the creation of a high-speed, shockless reaction wave. If these gradients are sufficiently large, a transition from the high speed reaction wave to a strong detonation occurs. Time-dependent generalizations of the spontaneous flame concept, where the evolution of each fluid particle is determined by integration along particle paths only, are derived for initial velocity and pressure disturbances under the assumption of slowly varying initial disturbances. The unsteady structure of the high-speed reaction wave arising due to reaction from initial non-uniformities is investigated for the moderate activation energy used.

1. Introduction

Non-uniformities in an explosive mixture can arise through a variety of physical mechanisms, for example by the non-uniform heating or compression of a combustible mixture. Zeldovich *et al.* (1970) investigated several aspects of the problem of reaction in non-uniformly disturbed fluids by studying the evolution of a chemical system subject to an initial linearly decreasing temperature disturbance in an otherwise uniform fluid. The reaction was found to proceed at different rates at different points due to the initial non-uniform distribution of temperature. For a sufficiently small disturbance amplitude, it was found that the reaction of the system resulted in the creation of a high-speed, shockless reaction wave with the structure of a classical weak detonation (Fickett & Davies 1979). The reaction wave consisted of a locus of non-uniform ignition times, where self-ignition of each fluid particle occurred non-simultaneously in each fluid volume as a result of the weakly varying, but nevertheless non-uniform initial temperature disturbance. By increasing the amplitude of the initial temperature disturbance, thereby generating a strong reactive-compressible coupling between local gas-dynamic effects and exothermic chemical energy release during the evolution, it was found that the initially high-speed reaction wave would slow below the Chapman–Jouguet detonation velocity appropriate to the initial state of the material. At this stage, it could no longer sustain its shockless structure and a transition to a conventional strong detonation was seen to result. These investigations have also been extended to systems in which high-speed reaction waves are generated

Phil. Trans. R. Soc. Lond. A (1995) **353**, 173–203
Printed in Great Britain

from non-uniform gradients in the initial reactant mass concentration (e.g. Gel'fand *et al.* 1985; Zeldovich *et al.* 1988).

Several theoretical asymptotic approaches have offered explanations for the evolution connected with this kind of detonation initiation. Bdzil & Kapila (1992) were able to derive the structure of the high-speed reaction wave under the assumption that the wave is essentially quasi-steady in an appropriate reference frame. In addition, they were able to describe the evolution to a strong detonation which results when the high-speed reaction wave slows below the Chapman–Jouguet detonation velocity appropriate to the initial state of the material. Dold & Kapila (1995*a*, *b*) provided a formal asymptotic description under the assumption of high activation energy of the transition from a non-uniformly disturbed fluid, to the generation of a quasi-steady supersonic shockless reaction wave, and the subsequent emergence of a strong detonation.

An *ad hoc* method for the study of the properties of high-speed reaction waves arising from non-uniformly disturbed fluids has been proposed by Zeldovich (1980). It was assumed that the path of these flames could be constructed as a series of adiabatic explosions, relative to the initial state of each fluid particle. Thus each particle in the system is assumed to react at constant volume independently of the behaviour of neighbouring particles. For a one-step Arrhenius reaction with initial heterogeneities in temperature and concentration, it is straightforward to construct a locus of constant volume ignition times, which depend on the initial state only, that would then make up the path of the so-called *spontaneous flame* (Gel'fand *et al.* 1985). Since this concept ignores the gas-dynamic interaction between neighbouring fluid particles, and therefore the evolution of each particle is purely time-dependent, it provides a useful basis upon which to study the properties of high-speed reaction waves.

In most practical systems, it is unlikely that non-uniformities only in the temperature and reaction mass fraction distributions will exist. Non-uniform distributions in pressure and velocity are also likely to be present. The dynamic effect of such disturbances is to induce localized volumetric expansions or compressions, which in a reactive fluid will then act to accelerate or oppose the local rate of chemical reaction as kinetic flow energy is distributed within the material. As such, initial non-uniformities in velocity and pressure alone might then be expected to induce gradients in the spatial distribution of ignition times, leading to the generation of high-speed reaction waves. Hence the possibility of transition to a conventional strong detonation for such disturbances with sufficiently large amplitudes can be realized. In any reactive system involving initial non-uniformities, it is clearly important to be able to predict the effects of initial velocity and pressure non-uniformities on the possible evolution of a detonation in the system. Associated with the ignition aspect of this important problem, there have been a number of high-activation energy studies on the ignition of an initially homogeneous medium disturbed by a short-wavelength small-amplitude acoustic pulse (Clarke 1979; Blythe 1978; Almgren 1992) and by similar waves propagating in opposite directions (Stewart 1986, 1988; Majda & Rosales 1987; Almgren 1992). One of the conclusions arising from this work is that the presence of initial pressure and velocity disturbances can have equally as dramatic an effect on the evolution of a reactive atmosphere as initial disturbances in temperature and reactant mass concentration.

In the following work, an investigation is presented into the evolution of a reactive atmosphere using a one-step chemical model with a moderate, realistic, activation

PHILOSOPHICAL TRANSACTIONS OF THE ROYAL SOCIETY A MATHEMATICAL, PHYSICAL & ENGINEERING SCIENCES

energy subject to small-amplitude non-uniform velocity, pressure, temperature and larger-amplitude reactant mass fraction disturbances with wavelengths on the order of an appropriate acoustic scale. The numerical solutions are obtained through a standard finite-difference Lax–Wendroff solution of the reactive Euler system of equations incorporating artificial viscosity. For the moderate activation energy used in the present study, this basic method of solution is found to provide an adequate resolution of the evolution to detonation from an initially disturbed medium. An asymptotic derivation of the spontaneous flame concept (Zeldovich 1980) is also presented under the assumption of slowly varying initial disturbances. This assumption allows for a generalization of the spontaneous flame concept which accounts for the presence of initial velocity and pressure disturbances. In the spirit of Zeldovich's original formulation, the evolution of any fluid element is still described by time-dependent integration along a particle path only, subject to the initial state of the particle. In addition, it is demonstrated that the structure of the high-speed reaction wave found to arise for reaction from initial conditions using a realistic moderate activation is unsteady and similar to the unsteady flame structure recently found by Singh & Clarke (1992) in a piston-shock configuration.

2. Model

The explosive is modelled as a polytropic fluid which undergoes a one-step mole preserving reaction of the form,

$$\mathrm{F} \rightarrow \mathrm{P},$$

which converts reactant species F into product species P with the liberation of Q^* units of energy per unit mass of reactant. Here, all dimensional and unscaled quantities are signified by the addition of an asterisk to the appropriate symbol. The mass rate of consumption of F per unit volume is assumed to follow an Arrhenius rate law. In addition it is assumed that the material is sufficiently hot initially such that conduction processes, which evolve on the scale of a local diffusion time, play no role in determining the chemical evolution of the system, which instead is determined by an interaction between compressible gas-dynamics and exothermic chemistry.

(*a*) *Equations and chemical model*

The dimensionless Eulerian equations of reactive motion can be written in a one-dimensional mass-weighted Lagrangrian system as follows:

$$\left.\begin{aligned} V_t - \delta U_\chi = 0, \quad U_t + \delta\gamma^{-1}P_\chi = 0, \quad T = PV, \\ T_t - \frac{\gamma-1}{\gamma}VP_t = -Qy_t, \quad Qy_t = -\frac{y}{\beta}\exp\left(\beta\left(1-\frac{1}{T}\right)\right). \end{aligned}\right\} \tag{2.1}$$

The variables T, P, V, U and y are the non-dimensional temperature, pressure, specific volume, fluid velocity and scaled reactant mass fraction respectively. The non-dimensionalization of T^*, P^*, V^* and scaling of y^* are taken with respect to the fluid state at the reference location $x^* = \hat{x}^*$, such that $T = T^*/\widehat{T}^*$, $P = P^*/\widehat{P}^*$, $V = V^*/\widehat{V}^*$ and $y = y^*/\hat{y}^*$. The time $t = t^*/t_{\mathrm{r}}^*$ is scaled with respect to the homogeneous

constant pressure induction time t_{r}^* at $\hat{x}^*$, where

$$t_{\mathrm{r}}^* = \frac{1}{A^*} \frac{C_p^* \widehat{T}^*}{Q^* \hat{y}^*} \frac{\widehat{T}^*}{T_A^*} \mathrm{e}^{T_A^*/\widehat{T}^*} \tag{2.2}$$

for pre-exponential Arrhenius factor A^*, specific heat at constant pressure C_p^* and activation temperature T_A^*.

For a given initial disturbance, the characteristic length scale l_{r}^* is taken to represent a distance over which comparable rates of chemical reaction are distributed initially relative to the reference point. A non-dimensional distance x is then given by $x = x^*/l_{\mathrm{r}}^*$, and a reference acoustic time t_{a}^* can then be defined as

$$t_{\mathrm{a}}^* = l_{\mathrm{r}}^*/\sqrt{(\gamma \widehat{P}^* \widehat{V}^*)}, \tag{2.3}$$

identifying the time an acoustic disturbance would take to propagate the distance l_{r}^*. The parameter δ appearing in the equations (2.1) above is defined as the ratio of the reference induction time t_{r}^* to the reference acoustic time t_{a}^*, i.e.

$$\delta = t_{\mathrm{r}}^*/t_{\mathrm{a}}^* \tag{2.4}$$

and represents the relative effects of compressibility in the evolution. If the characteristic wavelength of the initial disturbance is such that $\delta = 1$, then a strong reactive-compressible coupling between the gas-dynamic evolution and the chemical reaction results. On the other hand, if the initial disturbance is sufficiently slowly varying in space, such that $\delta \ll 1$, then the evolution is dominated by a constant volume chemical evolution. Changes in the fluid velocity are assumed to occur on the scale of the local sound speed, so that a non-dimensional velocity can then be defined as $U = U^*/\sqrt{(\gamma \widehat{P}^* \widehat{V}^*)}$. The remaining dimensionless constants appearing above are the activation energy $\beta = T_A^*/\widehat{T}^*$, the heat release factor $Q = Q^* \hat{y}^*/C_p^* \widehat{T}^*$ and the adiabatic coefficient γ. The non-dimensional Lagrangrian mass coordinate χ is defined as

$$\chi = \int_{x_0(t)}^{x} \frac{\mathrm{d}x}{V}, \tag{2.5}$$

where the origin of the mass-weighted coordinate frame ($\chi = 0$) is chosen to move along a path traced out by a particle with the fluid velocity $\mathrm{d}x_0(t)/\mathrm{d}t = U$ whose initial location is given at $x = \hat{x} = x_0(0)$ with $U = \widehat{U}$. Finally, it is useful to re-arrange the energy, mass and gas-state equations to give the two equations,

$$\gamma^{-1} V P_t = -Q y_t - \delta P U_\chi, \quad T_t = -\gamma Q y_t - \delta(\gamma - 1) P U_\chi, \tag{2.6}$$

which describe how local exothermic chemical energy release is distributed between temperature and pressure increase and the kinetic energy of local expansion and compression of the fluid.

(*b*) *Initial conditions*

The solution of equations (2.1) will be investigated subject to a set of initial fluid and reactant mass fraction non-uniformities at $t = 0$ which in their most general form can be written as

$$T = T_i(\chi), \quad P = P_i(\chi), \quad V = V_i(\chi), \quad U = U_i(\chi) \quad \text{and} \quad y = y_i(\chi). \tag{2.7}$$

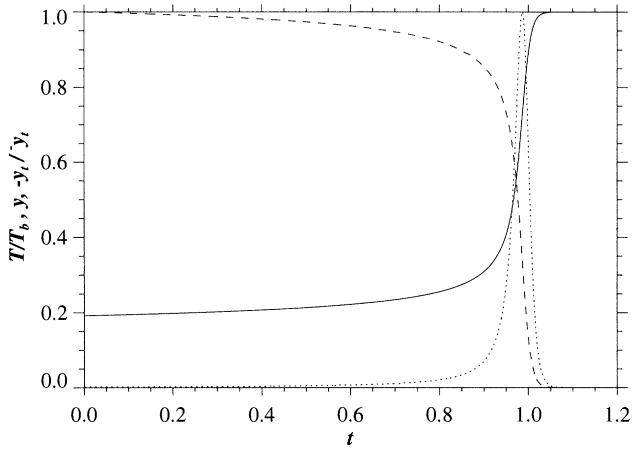

Figure 1. Variation of normalized temperature T/T_b (solid line), reactant mass fraction y (dashed line) and normalized reactant consumption rate $-y_t/\bar{y}_t$ (dotted line) against time t for a reaction arising from the uniform initial state (3.1) with $Q = 3$, $\gamma = 1.4$ and $\beta = 10$. The normalizing factors are the burnt temperature $T_\mathrm{b} = 5.2$, and maximum reactant consumption rate $\bar{y}_t = 17.61$.

(*c*) *Non-reactive evolution*

In a non-reactive system the second of equations (2.1) and the first of equations (2.6) can be combined into the characteristic form,

$$\gamma^{-1}(P_t \pm \alpha P_\chi) \pm \alpha(U_t \pm \alpha U_\chi) = 0, \tag{2.8}$$

when $\delta = 1$. When the fluid is disturbed, the two characteristic quantities $\gamma^{-1}P - \alpha U$ and $\gamma^{-1}P + \alpha U$ radiate as leftwards and rightwards-propagating waves respectively along the paths $\partial\chi/\partial t = \pm\alpha$, where

$$\alpha = \sqrt{P/V} \tag{2.9}$$

is the acoustic impedance or the chemically frozen rate of propagation of an acoustic disturbance in χ-space. From the second of equations (2.6) with $\delta = 1$ it can also be seen that the temperature variation in a non-reactive material is determined according to the relation

$$T_t = -(\gamma - 1)PU_\chi. \tag{2.10}$$

The temperature decreases locally ($T_t < 0$) whenever $U_\chi > 0$ as heat is lost to the kinetic energy of expansion of the gas. Similarly, the temperature increases locally ($T_t > 0$) wherever there is a local flow compression, i.e. where $U_\chi < 0$. Differing rates of flow divergence U_χ correspond to differing local flow kinetic energies and thus imply non-uniform rates of temperature variation within the fluid.

3. Reaction from uniform initial conditions

For an initially homogeneous explosive at rest with the uniform initial conditions

$$T_i(\chi) = P_i(\chi) = V_i(\chi) = y_i(\chi) = 1 \quad \text{and} \quad U_i(\chi) = 0, \tag{3.1}$$

it can be shown from equations (2.1) with $\delta = 0$ that the spatially uniform temperature at any time t can be described by the integral equation

$$t = \frac{\beta}{\gamma}\int_1^T \left[1 - \frac{(T-1)}{\gamma Q}\right]^{-1} \exp\left[-\beta\left(1 - \frac{1}{T}\right)\right] \mathrm{d}T \tag{3.2}$$

together with the relations for y, P, U and V as

$$y = 1 - (T-1)/\gamma Q, \quad P = T/V, \quad U = 0 \quad \text{and} \quad V = 1. \tag{3.3}$$

For sufficiently large activation energies, Kassoy (1975) has given an asymptotic description of the solution to (3.2) from reaction initiation to reaction completion. For a moderate activation energy $\beta = 10$, figure 1 shows the variation in normalized temperature, reactant mass fraction and normalized rate of reactant consumption with time for a homogeneous explosion with $Q = 3$, $\gamma = 1.4$. The figure illustrates the presence of a quiescent initial induction stage, where in a time $t = 0.847$ only a tenth of the reactant has been consumed. The maximum rate of reactant consumption $\bar{y}_t = \max\{|y_t|\}$ occurs for general Q, γ and β when $y = \bar{y}$ has the value,

$$\bar{y} = (1 + (1+\beta/2)/Q\gamma) + \sqrt{(1 + (1+\beta/2)/Q\gamma)^2 - (1+Q\gamma)^2/Q^2\gamma^2}. \tag{3.4}$$

For $Q = 3$, $\gamma = 1.4$ and $\beta = 10$, $\bar{y} = 0.34$ and the corresponding fluid temperature is given by $T = \overline{T} = 3.78$. This point in the evolution is reached at the time $t = \bar{t} = 0.986$. From the last of equations (2.1), the maximum reactant consumption rate is then given by $\bar{y}_t = 17.61$ when approximately two thirds of the reactant has been consumed. Finally, the time at which the reactant is almost depleted, evaluated here when $y = 10^{-2}$, is calculated to be $t = 1.0263$. The corresponding temperature at this point is given by $T = 5.158$, which is close to the burnt temperature $T_\mathrm{b} = 5.2$.

Due to the nature of the Arrhenius reaction rate, a moderate activation energy of $\beta = 10$, as used above, will result in a substantially thicker reaction zone in comparison with that arising during a homogeneous explosion with a higher activation energy of $\beta = 15$. This is due to the exponential dependence of the reaction rate on the activation energy. For the former case, 80% of the chemical energy released into the system associated with the reactant depletion $0.9 \geqslant y \geqslant 0.1$ occurs during the time $0.847 \leqslant t \leqslant 1.003$. This constitutes about 1/7 of the reaction time $t = 1.0263$ where $y = 10^{-2}$. In the latter case an identical amount of reactant depletion $0.9 \geqslant y \geqslant 0.1$ occurs during the time $0.832 \leqslant t \leqslant 0.8589$, which is about 1/32 of the reaction time $t = 0.8596$ where $y = 10^{-2}$. The maximum reactant consumption rate associated with the case $\beta = 15$ is given by the value $\bar{y}_t = 490.10$ which occurs at the time $t = \bar{t} = 0.8585$ with $y = \bar{y} = 0.265$ and $T = \overline{T} = 4.086$. Consequently the lower activation energy of $\beta = 10$ constitutes a process with a significantly slower rate of chemical energy release into the system during ignition. As will be demonstrated later, the use of moderate activation energies can then have a major influence on the structure of the reaction waves which arise from reaction in a non-uniformly disturbed medium.

4. Evolution from slowly varying initial perturbations

If the initial conditions (2.7) are slowly varying in space, such that the reference time t_r^* is much shorter than the acoustic time t_a^* associated with the initial distur-

PHILOSOPHICAL TRANSACTIONS OF THE ROYAL SOCIETY A MATHEMATICAL, PHYSICAL & ENGINEERING SCIENCES

bance, a solution of equations (2.1) can be obtained under the asymptotic limit

$$\delta \ll 1. \tag{4.1}$$

This procedure determines the resulting changes to the homogeneous explosion problem which results from the presence of weak initial disturbances. In order to determine the evolution of the temperature and reactant mass fraction asymptotically to $O(\delta^3)$, expansions for T, P, V, and y are taken in the form

$$\mathcal{F}(\chi, t; \delta) = \mathcal{F}_0(\chi, t) + \delta \mathcal{F}_1(\chi, t) + \delta^2 \mathcal{F}_2(\chi, t) + O(\delta^3) \tag{4.2}$$

and for U in the form,

$$U(\chi, t; \delta) = U_0(\chi, t) + \delta U_1(\chi, t) + O(\delta^2). \tag{4.3}$$

Substituting expansions (4.2) and (4.3) into equations (2.1), the following equations are derived at leading order:

$$V_{0t} = 0, \quad U_{0t} = 0, \quad T_{0t} = -\gamma Q y_{0t}, \quad Q y_{0t} = -\frac{y_0}{\beta} \exp\left(\beta\left(1 - \frac{1}{T_0}\right)\right), \quad P_0 = \frac{T_0}{V_0}, \tag{4.4}$$

which, with the initial conditions (2.7), have the solution,

$$\left.\begin{aligned} V_0 = V_i(\chi), \quad U_0 = U_i(\chi), \quad y_0 = y_i(\chi) + (T_i(\chi) - T_0)/\gamma Q, \quad P_0 = T_0/V_i(\chi), \\ T_{0t} = \frac{\gamma}{\beta}(y_i(\chi) - \frac{T_0 - T_i(\chi)}{\gamma Q}) \exp\left(\beta\left(1 - \frac{1}{T_0}\right)\right). \end{aligned}\right\} \tag{4.5}$$

Thus at leading order, Zeldovich's notion of a spontaneous flame is recovered (Zeldovich 1980). Each particle evolves independently of neighbouring fluid elements and the evolution is determined purely in terms of the initial conditions by time-dependent integration along each particle path. At this order, for a uniform initial temperature and reactant mass concentration, a homogeneous evolution for temperature and reactant mass concentration results and initial velocity and pressure disturbances do not affect the evolution. At $O(\delta)$, the corrections for velocity U_1 and specific volume V_1 are determined through the equations,

$$V_{1t} = U_i'(\chi), \quad U_{1t} = -\gamma^{-1} \frac{\partial}{\partial \chi}\left(\frac{T_0}{V_i}\right), \quad \text{where} \quad V_1 = 0, \quad U_1 = 0 \quad \text{at} \quad t = 0. \tag{4.6}$$

These have the solution,

$$V_1 = U_i'(\chi) t, \quad U_1 = -\gamma^{-1} \int_0^t \frac{\partial}{\partial \chi}\left(\frac{T_0}{V_i}\right) \mathrm{d}t. \tag{4.7}$$

At $O(\delta^2)$, the specific volume correction is determined through the equation,

$$V_{2t} = -\gamma^{-1} \int_0^t \frac{\partial^2}{\partial \chi^2}\left(\frac{T_0}{V_i}\right) \mathrm{d}t, \quad \text{where} \quad V_2 = 0 \quad \text{at} \quad t = 0, \tag{4.8}$$

with solution

$$V_2 = -\gamma^{-1} \int_0^t \int_0^t \frac{\partial^2}{\partial \chi^2}\left(\frac{T_0}{V_i}\right) \mathrm{d}t\, \mathrm{d}t. \tag{4.9}$$

Explicit differential relations for the temperature and reactant mass fraction corrections terms could be written down at this stage, but it transpires that it is simplest

to combine the leading order terms T_0 and y_0 with the correction terms T_1, T_2 and y_1, y_2 to give the expressions for temperature and reactant mass concentration

$$T_t = -\gamma Q y_t - \delta(\gamma-1)T\frac{U_i'(\chi)+\delta U_{1\chi}}{V_i(\chi)+\delta V_1}, \quad Qy_t = -\frac{y}{\beta}\exp\left(\beta\left(1-\frac{1}{T}\right)\right), \tag{4.10}$$

which determine T and y to $O(\delta^3)$. The expressions for V_1 and U_1 are given by (4.7). Finally, the pressure is determined from the equation

$$P = \frac{T}{V_i + \delta V_1 + \delta^2 V_2} \tag{4.11}$$

to $O(\delta^3)$. Thus by determining the leading order solution (4.5) with corrections (4.7) and (4.9), numerical quadrature of equations (4.10) determine the evolution of temperature and reactant mass concentration to $O(\delta^3)$. For a uniform initial temperature disturbance, the subsequent evolution of temperature then depends on initial velocity and pressure disturbances.

5. Evolution of a reactive atmosphere with an initial velocity disturbance

(*a*) *The spontaneous flame for initial velocity disturbances*

Under Zeldovich's concept of a spontaneous flame (Zeldovich 1980), it was proposed that a path of ignition arising from an initial disturbance could be estimated by assuming that each fluid particle evolves uniformly as though surrounded by fluid particles with the same initial state. Thus the gasdynamic interaction between neighbouring particles is completely neglected. This definition does not account for initial velocity disturbances since the ignition of a region of fluid particles is unaffected by a local uniform distribution in velocity. However, under the assumption of slowly varying initial disturbances, a generalization of the spontaneous flame concept has been made above to model the effects of an initial velocity disturbance. Consider the initial fluid state consisting of a disturbance in velocity only,

$$U = U_i(\chi), \quad T_i(\chi) = P_i(\chi) = V_i(\chi) = y_i(\chi) = 1. \tag{5.1}$$

If the disturbance is slowly varying, then $\delta \ll 1$ and the evolution is determined by the asymptotic analysis presented in § 4. Since $T_i(\chi) = y_i(\chi) = V_i(\chi) = 1$, then from the fourth of equations (4.5) $T_0 = T_0(t)$, and from (4.7) and (4.9) $U_1 = V_2 = 0$. Thus the evolution to $O(\delta^3)$ is determined by the equations

$$\left.\begin{aligned} &U = U_i(\chi), \quad V = 1+\delta U_i'(\chi)t, \quad P = T/(1+\delta U_i'(\chi)t), \\ &T_t = -\gamma Q y_t - \delta(\gamma-1)\,T\,\frac{\delta U_i'(\chi)}{(1+\delta U_i'(\chi)t)}, \quad -Qy_t = \frac{y}{\beta}\exp\left(\beta\left(1-\frac{1}{T}\right)\right). \end{aligned}\right\} \tag{5.2}$$

Thus each fluid element evolves as though surrounded by fluid particles having the same rate of compression or expansion. In the spirit of Zeldovich's formulation, each particle evolves independently of neighbouring particles, i.e. the behaviour of each particle is determined by integration along particle paths, and depends only on time and the initial fluid divergence rate $U_i'(\chi)$. It should also be noted that whilst the solution (5.2) is valid for slowly varying disturbances, they are exact for initial linear

velocity profiles of the form $U_i(\chi) = -b\chi$ for constant b. Generally, at any point $\chi = \widehat{\chi}$ the evolution is determined by the numerical quadrature of equations (5.2) with initial conditions (5.1). The last term on the right-hand side of the fourth of equations (5.2) is either a source or sink term for the fluid temperature of each particle brought about by the presence of the initial velocity disturbance.

For a general initial flow disturbance (5.1), the term $-\delta(\gamma-1)TU_i'/(1+\delta U_i't)$ slows the rate of increase of temperature T_t at points where $U_i'(\chi) > 0$. Relative to a uniform explosion where $U_i'(\chi) = 0$, the initial fluid expansion hinders the rate of increase of temperature by locally extracting heat from the region. Consequently, one should expect a reaction time greater than the appropriate static reaction time where $U_i'(\chi) = 0$. The opposite applies to initial flow compressions, $U_i'(\chi) < 0$, where the kinetic term $-\delta(\gamma-1)TU_i'(\chi)/(1+\delta U_i'(\chi)t)$ assists the rate of increase of temperature T_t. Relative to a uniform explosion the compression acts to accelerate the rate of increase of temperature by contributing kinetic flow energy in addition to the release of chemical energy. The fourth of equations (5.2) also shows that the larger the magnitude of $|U_i'(\chi)|$ the more dominant the relative effect generated by the initial velocity non-uniformity. At points where $\delta U_i'(\chi) > \gamma/\beta(\gamma-1)$ the temperature falls initially, since the energy extracted by the initial expansion is greater than the energy release due to chemical reaction.

(*b*) *Numerical computation of the evolution from a periodic initial velocity disturbance*

In order to illustrate the typical influence of an unsteady evolution generated by an initial small amplitude velocity disturbance on establishing a gradient of ignition times, consider the periodic initial distribution at $t = 0$,

$$U_i(\chi) = \frac{\nu}{\beta}\cos\left(\frac{\pi}{2\mu}(\chi+\mu)\right), \quad T_i(\chi) = P_i(\chi) = V_i(\chi) = y_i(\chi) = 1 \text{ for } 0 \leqslant \chi \leqslant 2\mu. \tag{5.3}$$

The temperature, pressure, specific volume and reaction mass fraction are all assumed to be in a state of initial homogeneity. The initial sinusoidal velocity perturbation has amplitude $2\nu/\beta$ and half-wavelength 2μ. The divergence rates of the initial velocity disturbance are given by

$$U_i'(\chi) = -\frac{\pi\nu}{2\mu\beta}\sin\left(\frac{\pi}{2\mu}(\chi+\mu)\right), \tag{5.4}$$

so that for $\nu > 0$, the disturbance will initially induce a local volumetric compression (where $U_i'(\chi) < 0$) in the fluid for $0 \leqslant \chi \leqslant \mu$, and a local volumetric expansion (where $U_i'(\chi) > 0$) for $\mu \leqslant \chi \leqslant 2\mu$. The points of initial maximum fluid compression and expansion rates lie respectively at $\chi = 0$ and $\chi = 2\mu$.

Figure 2 illustrates the effect of the initial velocity disturbance on the behaviour of the fluid velocity $U(\chi, t)$ and volume $V(\chi, t)$ respectively during ignition of the fluid particle at $\chi = 0$ for a finite-difference Lax–Wendroff numerical solution of equations (2.1) from the initial perturbation (5.3) with the parameters $\nu = 1$, $\mu = 0.75$, $Q = 3$, $\gamma = 1.4$ and $\beta = 10$ at the stated times. Figure 3*a* illustrates the full evolution of the temperature T and the reaction mass fraction y for $0 \leqslant \chi \leqslant 2\mu$ with $\nu = 1$, $\mu = 0.75$, $Q = 3$, $\gamma = 1.4$ and $\beta = 10$ at the stated times. Figures 3*b*–*e* show the corresponding evolution of the fluid pressure P, velocity U, specific volume V and reactant mass consumption rate $-y_t$ respectively. As is the case for larger activation

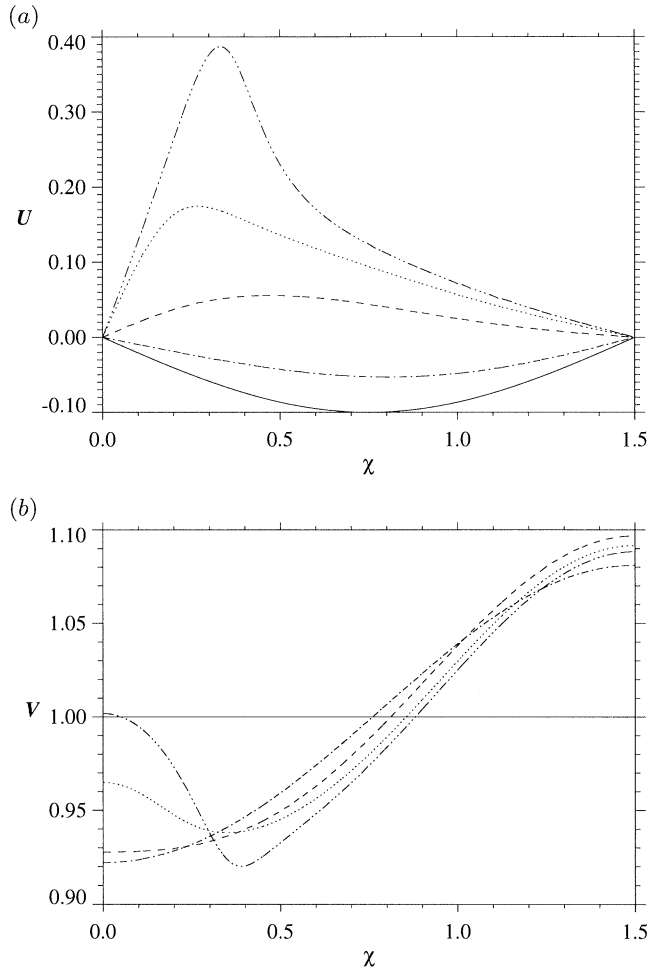

Figure 2. (a) The temporal evolution of the fluid velocity $U(\chi, t)$ and (b) volume $V(\chi, t)$ during ignition at $\chi = 0$ from the initial disturbance (5.3) for $Q = 3$, $\gamma = 1.4$ and $\beta = 10$ with $\nu = 1$ and $\mu = 0.75$ plotted at the times $t = 0.$ (solid line), $t = 0.45$ (dot-dash line), $t = 0.75$ (dashed line), $t = 0.83$ (dotted line) and $t = 0.86$ (dot-dot-dot-dash line).

energies, the early evolution is characterized by a chemical induction period, where the temperature and pressure rise is small. The variation of temperature $T = 1$ to $T = 1.8$ at $\chi = 0$ occurs in a time $t = 0.77$. The temperature and pressure rise and reactant concentration fall occur most rapidly at $\chi = 0$, where the initial maximum rate of fluid compression induced by the initial velocity disturbance exists. Ignition first occurs at $\chi = 0$, where reaction is almost complete ($y = 10^{-2}$) in the time $t \approx 0.86$. This reaction time is substantially reduced from that of the homogeneous reaction time of $t_I \approx 1.02$ for $\beta = 10$, since the initial fluid compression has generated an acceleration of reaction rates at $\chi = 0$ relative to the homogeneous ($U_i'(\chi) = 0$) reaction rates found for reaction from initial conditions (3.1). From figure 2 it is seen that the onset of significant chemical reaction as ignition occurs leads to a local expansion of gas around $\chi = 0$, generating a density maximum in the interior of the fluid.

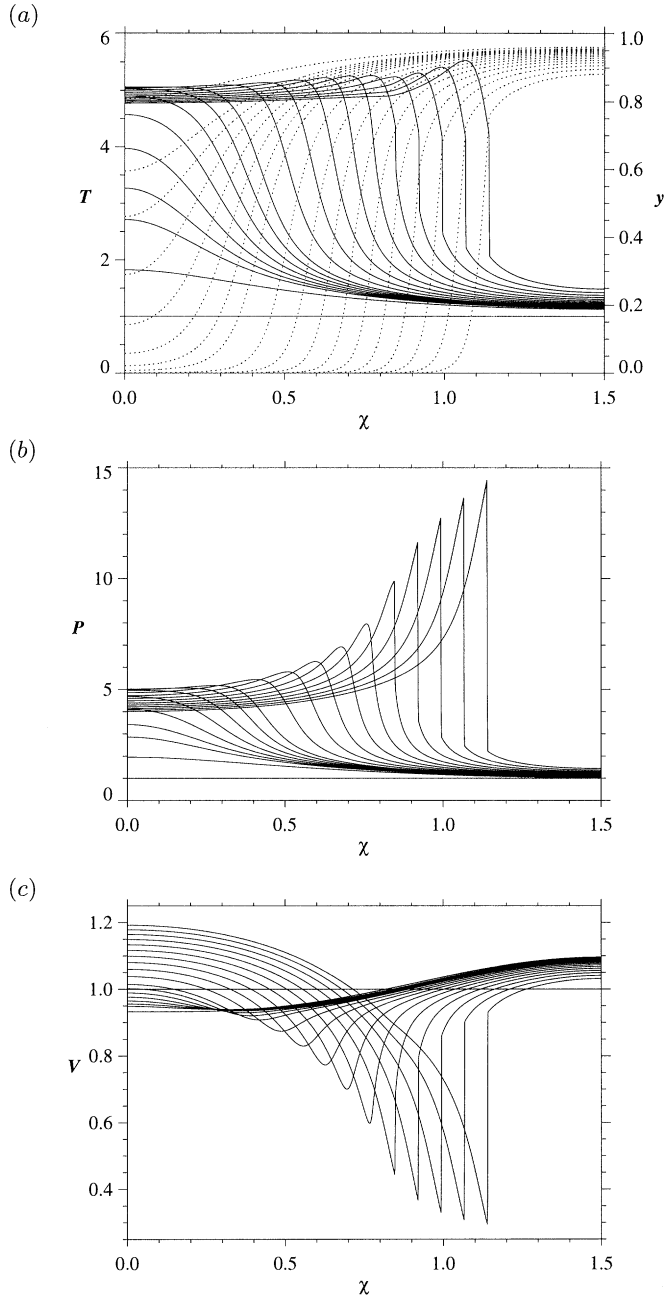

Figure 3. The evolution from initial disturbance (5.3) for $Q = 3$, $\gamma = 1.4$ and $\beta = 10$ with $\nu = 1$ and $\mu = 0.75$ for (a) temperature T (solid lines) and reactant mass fraction y (dotted lines), (b) pressure P, (c) specific volume V.

After ignition at $\chi = 0$ ($t > 0.86$), a reaction wave is generated due to the successive ignition of neighbouring fluid layers at different times induced by the effects of the initial non-uniform velocity distribution. It is seen that particles with an initially lower magnitude of compression react at progressively later times. This is precisely

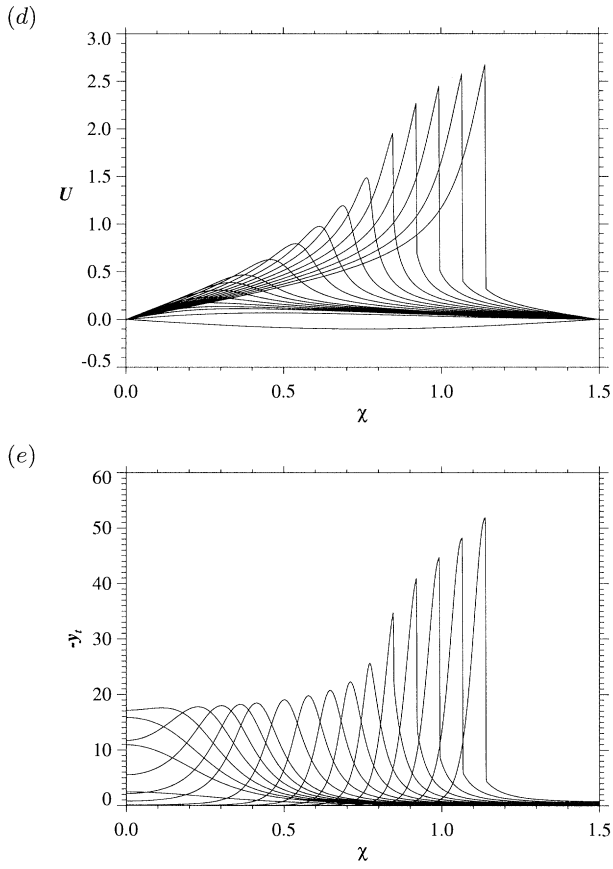

Figure 3. The evolution from initial disturbance (5.3) for $Q = 3$, $\gamma = 1.4$ and $\beta = 10$ with $\nu = 1$ and $\mu = 0.75$ for (d) fluid velocity U, and (e) reactant consumption rate $-y_t$ at the times $t = 0$, $t = 0.77$, $t = 0.81$–0.87 (in steps of 1) and $t = 0.89$–1.07 (in steps of 2).

the effect predicted above for the case of slowly varying initial disturbances. As time proceeds, higher pressure peaks are generated within the reaction wave and the gradients of all profiles gradually steepen within the wave as it moves forward. By the time $t = 0.99$ a weak reaction shock is seen to have formed within the reaction wave, characterized at this early stage by the thermodynamic pressure jumps $5 \lesssim P \lesssim 9.5$. Interestingly, from figure 3a it is seen that the shock appears in the middle of the reaction wave where $y \approx 0.475$. For $t > 0.99$, the reaction shock strengthens as it moves through the reaction zone and at time $t = 1.07$ the shock is located at $y = 0.76$ having a shock strength determined by the thermodynamic pressure jump $2 \lesssim P \lesssim 14.5$. The maximum gas pressure at this stage is approximately three times greater than that found behind the reaction wave first formed at $t = 0.87$. The Von-Neumann shock pressure corresponding to a Chapman–Jouguet propagating in the uniform atmosphere with $Q = 3$ is $P_N = 18.9$. Figure 3c, d demonstrates the presence of an expansion wave which follows the reaction wave structure for $t = 0.87$ to $t = 0.99$ to match the gas velocity at the end of the wave to that of $U = 0$ at $\chi = 0$. This expansion wave is then able to attach itself to the evolving strong detonation structure for $t > 0.99$ giving rise to the initial stages of a planar strong detonation structure propagating into a chemically evolving atmosphere.

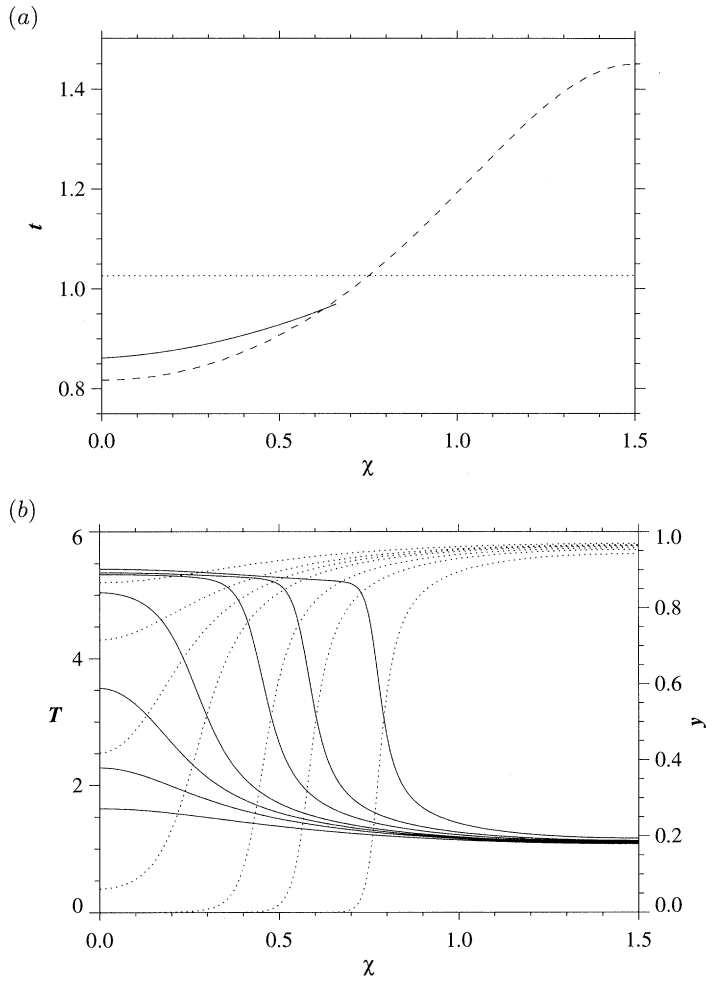

Figure 4. (*a*) A comparison of the numerically calculated ignition path where $y = 10^{-2}$ (solid line) with the spontaneous path calculated from equations (5.2) with $\delta = 1$ (dashed line) and an evolution with $U_i'(\chi) = 0$ (dotted line) and (*b*) the evolution of temperature and reactant mass fraction with constant fluid divergence shown at the times $t = 0.7$, $t = 0.75$, $t = 0.775$, $t = 0.8$, $t = 0.85$, $t = 0.9$ and $t = 1.0$ for an evolution from initial conditions (5.3) with $Q = 3$, $\gamma = 1.4$ and $\beta = 10$ with $\nu = 1$ and $\mu = 0.75$.

In figure 4*a* the locus of times where $y = 10^{-2}$ making up the path of the reaction wave before shock formation calculated numerically from the initial conditions (5.3) (solid line) with $\nu = 1$, $\mu = 0.75$, $Q = 3$, $\gamma = 1.4$ and $\beta = 10$ is compared with that obtained from the spontaneous evolution (5.2) (dashed line) with $\delta = 1$. The dotted line represents the uniform path of reaction points obtained when $U_i'(\chi) = 0$ and $y = 10^{-2}$. The spontaneous path predicts that relative to the static evolution where $U_i'(\chi) = 0$, ignition times are increased for $U_i'(\chi) > 0$ and decreased for $U_i'(\chi) < 0$. The spontaneous path predicts slighter lower reaction times for each particle than the numerical solution, however, the approximation for this particular example is clearly acceptable up to shock formation. The spontaneous evolution predicts a reaction time of $t_I \approx 0.82$ at $\chi = 0$, compared to the actual time of $t_I \approx 0.86$. Figure 4*b* shows the spatial evolution of temperature and reactant mass fraction as predicted by the

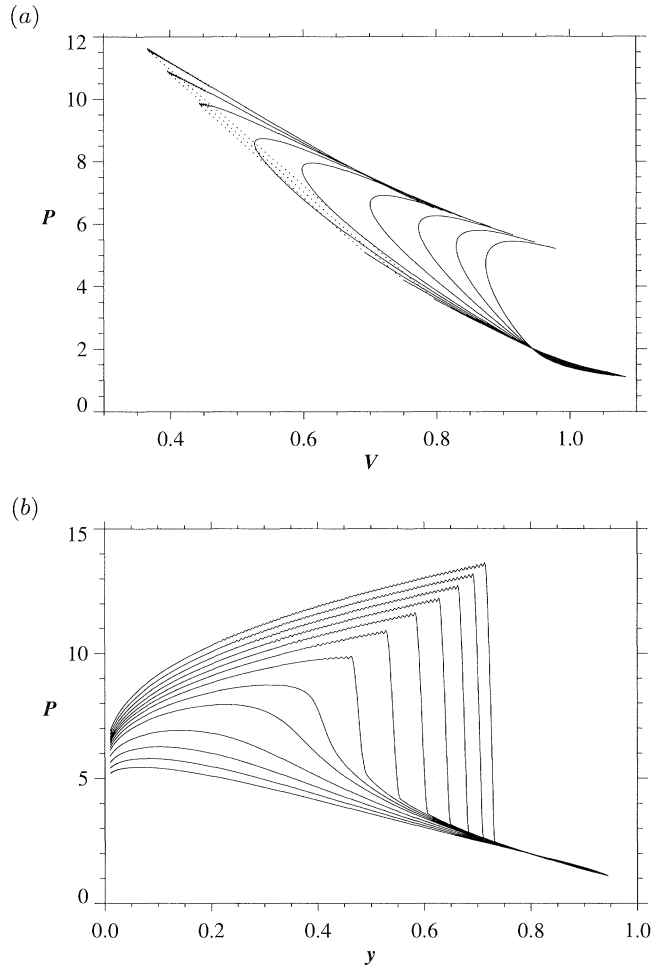

Figure 5. (*a*) Pressure–volume variation at $t = 0.89$–0.97 (in steps of 2) and $t = 0.98$–1.01 (in steps of 1) and (*b*) pressure-reactant mass fraction variation at $t = 0.89$–0.97 (in steps of 2) and $t = 0.98$–1.05 (in steps of 1) for the initial disturbance (5.3) for $Q = 3$, $\gamma = 1.4$ and $\beta = 10$ with $\nu = 1$, $\mu = 0.75$ and $1 \geqslant y(\chi, t) \geqslant 10^{-2}$. The dotted lines in (*a*) indicate the location of shock waves.

spontaneous evolution (5.2) with $\delta = 1$ at the times shown. Before the appearance of a reaction shock in the numerical solution, there are distinct similarities in the spatial aspects of the evolution.

(*c*) *The flame structure*

For sufficiently large activation energies ($\beta \gg 1$), Dold & Kapila (1995*a*) demonstrated that the reaction wave resulting from an initial small amplitude disturbance such as (5.3) should have a quasi-steady structure. On a pressure-volume diagram, these waves should then appear as straight lines. In addition, Dold & Kapila (1995*b*) showed that if the reaction slowed to the Chapman–Jouguet detonation velocity appropriate to the initial state of the material, then a sonic point appears at the end of reaction wave where $y = 0$. Any further slowing destroys the quasi-steady nature of the reaction wave and faster acoustic processes penetrate into the back of the wave

resulting in the formation of a weak reaction shock. The reaction shock is then amplified as it moves through the reaction wave, converting the structure to a classical strong detonation wave with Zeldovich–Döring–Von Neumann structure (Fickett & Davies 1979).

Figures 5*a* and *b* respectively show the pressure-volume ($P-V$) variation and pressure-reactant mass fraction variation ($P-y$) for $y \geqslant 10^{-2}$ which arise for $Q=3$, $\gamma=1.4$ and $\beta=10$ from the initial velocity disturbance (5.3) with $\nu=1$ and $\mu=0.75$ for $0 \leqslant \chi \leqslant 2\mu$ at the evolution times shown. Before reaction shock formation, the flame structure arising for reaction from initial conditions (5.3) with the moderate activation energy $\beta=10$ show distinct similarities to the unsteady structure found by Singh & Clarke (1992) on the analysis of the evolution of a reactive-compressible atmosphere behind a piston-driven shock wave using a moderate activation energy. It does not behave in the quasi-steady manner predicted by Dold & Kapila (1995*a*).

The P–V variation (figure 5*a*) demonstrates the presence of three different chemical regimes which make up the flame structure at any one stage before the onset of reaction shock formation. Detailed analysis and descriptions of these regimes have been presented by Singh & Clarke (1992) and to avoid repetition only brief details are given here. Attached to an evolving unsteady induction zone there is a quasi-steady, partially burnt, locally supersonic reaction regime, the properties of which are closely associated with the structure of a weak detonation where pressure increases through the wave while the fluid volume decreases as chemical reactant is consumed. Thus the head of the reaction wave moves forward supersonically. Dold & Kapila (1995*a*) predict that for high activation energies the quasi-steady weak detonation comprises the complete reaction wave structure. However, for moderate activation energies the partially burnt weak detonation is terminated by an unsteady evolution which limits the rise in pressure. At the rear of the reaction zone is then a locally subsonic reaction wave with the structure of a fast flame (Clarke & Kassoy 1985) in which pressure decreases through the flame while the fluid volume increases.

Figure 5*b* demonstrates how reaction shock formation occurs within the reaction structure. With continued movement of the reaction wave, the subsonic fast flame structure at the rear of the reaction wave becomes more dominant. Reaction shock initiation appears to occur ahead of the fast flame structure due to the steepening effects brought about the nonlinear chemical enhancement of compression waves within the unsteady reaction zone (Dold *et al.* 1995). The reaction shock first forms between the times $t=0.98$ and $t=0.99$ for $y \approx 0.475$. The reaction shock then couples with the subsonic fast flame structure to generate the initial stages of a conventional strong detonation structure which, as shown in figure 5*b*, strengthens on moving through the weak detonation structure. This again contrasts with the shock initiation process predicted by Dold & Kapila (1995*a*), where the reaction shock is predicted to form at the rear of the reaction wave where $y=0$.

The main feature of the present study and that of Singh & Clarke (1992) is that there is considerable unsteady behaviour within the reaction wave arising as a result of the use of a realistic moderate activation energy. Consider any stage in the local ignition of a fluid particle, where $T=\widetilde{T}$, $P=\widetilde{P}$ and $V=\widetilde{V}$ for reactant concentration $y=\tilde{y}$. At this point the relative importance of compressibility effects to chemical effects is measured by the ratio,

$$\tilde{\delta} = t_{\mathrm{r}}^{*}/t_{\mathrm{a}}^{*}, \tag{5.5}$$

where t_{r}^{*} and t_{a}^{*} adopt the more general definitions than those given in § 2, appropriate

PHILOSOPHICAL TRANSACTIONS OF THE ROYAL SOCIETY A MATHEMATICAL, PHYSICAL & ENGINEERING SCIENCES

at $t = 0$, i.e.

$$t_{\mathrm{r}}^{*} = \frac{1}{\gamma}\int_{\widetilde{T}}^{T_{\mathrm{b}}} \frac{1}{\beta^{-1}[1-(T-T_i(\chi)/\gamma Q]\mathrm{e}^{\beta(1-1/T)}}\,\mathrm{d}T, \quad t_{\mathrm{a}}^{*} = \frac{l_{\mathrm{r}}^{*}}{\sqrt{(\gamma\widetilde{P}\widetilde{V})}}. \tag{5.6}$$

Then t_{r}^{*} represents the time remaining to complete reaction of the fluid particle and t_{a}^{*} represents the time taken for an acoustic disturbance to cross a region of size l_{r}^{*} in which the most significant chemical changes are occurring. If $\tilde{\delta} \ll 1$, then acoustic disturbances are unable to propagate to any significant degree against the rate of completion of chemical reaction in any one region and further chemical evolution occurs at almost fixed volume. However, if the ratio $\tilde{\delta} = O(1)$ occurs during the stages of significant reaction, then spatial changes will be important in determining the local evolution of the flame structure. Moreover, shock formation is now possible within the flame structure itself as a dependence on the nonlinear shock formation terms in the Euler equations (2.1) are retained in this limit. Thus although $\tilde{\delta}$ may be small in one part of the reaction for a particular particle, e.g. at $t = 0$, the limit $\tilde{\delta} = O(1)$ could arise elsewhere during the evolution. That this is more likely to occur for lower activation energies can be seen from considering the rates of maximum reactant consumption for $\beta = 10$ and $\beta = 15$ in a homogeneous explosion. For $\beta = 10$ (figure 1), the maximum reactant consumption rate achieved during the evolution has a value $\bar{y}_t = 17.61$. This situation changes substantially for an activation energy of $\beta = 15$, where the maximum reactant consumption rate achieved has a value $\bar{y}_t = 490.10$. Consequently, in a non-uniform evolution, the likelihood that the local time scale for the propagation of acoustic disturbances across the region of most significant chemical changes to be comparable to the local time-scale for the chemical changes to occur will be greater for $\beta = 10$ due to the slower rate of chemical reaction. In summary, for sufficiently high activation energies where $\beta \gg 1$, the reaction wave is predicted to have a quasi-steady structure, whilst for moderate activation energies involving a slower rate of chemical energy release, unsteady effects are prevalent in the reaction zone structure.

6. The evolution from an initial pressure disturbance

(*a*) *The spontaneous flame for initial pressure disturbances*

The presence of an initial pressure disturbance in an otherwise uniform fluid will generate a non-uniform distribution of reaction rates providing that the second derivative of the spatial disturbance is non-uniform. A non-uniform flow divergence is then established in the fluid, where

$$U_{\chi} = -\gamma^{-1}\int_0^t P_{\chi\chi}\,\mathrm{d}t. \tag{6.1}$$

As in § 5, a generalization of Zeldovich's spontaneous flame concept (1980) can be made to include the effects of an initial pressure disturbance under the assumption of a slowly varying initial disturbance. Consider the initial non-uniform pressure disturbance,

$$P = P_i(\chi), \quad T = T_i(\chi) = y_i(\chi) = 1, \quad U = U_i(\chi) = 0 \quad \text{and} \quad V = V_i(\chi) = 1/P_i(\chi). \tag{6.2}$$

Since $T_i(\chi) = y_i(\chi) = 1$, it follows from the fourth of equations (4.5) that $T_0 = T_0(t)$, and the velocity evolution is determined as

$$U = -\delta\gamma^{-1}P_i'(\chi)\int_0^t T_0(t)\,\mathrm{d}t \tag{6.3}$$

to $O(\delta^2)$. The divergence rates for $t > 0$ which are established by the pressure disturbance are then given by

$$U_\chi = -\delta^2\gamma^{-1}P_i''(\chi)\int_0^t T_0(t)\,\mathrm{d}t. \tag{6.4}$$

Accordingly, the fluid volume adopts the form

$$V = V_i(\chi) - \delta^2\gamma^{-1}P_i''(\chi)\int_0^t\int_0^t T_0(t)\,\mathrm{d}t\,\mathrm{d}t, \tag{6.5}$$

where it follows from equation (4.10) that the evolution of temperature and reactant mass fraction is determined as

$$\left.\begin{aligned} T_t &= -\gamma Q y_t + \delta^2\frac{(\gamma-1)}{\gamma}TP_i(\chi)P_i''(\chi)\int_0^t T_0(t)\,\mathrm{d}t,\\ -Qy_t &= \frac{y}{\beta}\exp\left(\beta\left(1-\frac{1}{T}\right)\right). \end{aligned}\right\} \tag{6.6}$$

In the spirit of Zeldovich's formulation (Zeldovich 1980), the behaviour of each particle is determined by integration along particle paths only, and depends only on time and the initial pressure disturbance $P_i(\chi)$ and the distribution of the second derivative $P_i''(\chi)$. In order to calculate the evolution at any $\chi = \widehat{\chi}$ with time, the equations (6.6) are solved simultaneously with the initial conditions (6.2) with $P_i(\widehat{\chi})$ and $P_i''(\widehat{\chi})$ known. The last term of the first of equations (6.6) is either a source or sink term for the fluid temperature of each particle brought about by the presence of the initial pressure disturbance.

The relations (6.3)–(6.6), valid for slowly varying initial disturbances, demonstrate the underlying effects of an initial pressure disturbance. In regions where $P_i''(\chi) < 0$, a positive divergence rate

$$U_\chi = -\delta^2\gamma^{-1}P_i''(\chi)\int_0^t T_0(t)\,\mathrm{d}t > 0$$

is established and the kinetic term $-(\gamma-1)TU_\chi/V$ associated with the fluid expansion slows the rate of increase of temperature T_t. Relative to a homogeneous explosion where $P_i''(\chi) = 0$, one should then expect an increase in local ignition times. The opposite applies to initial flow compressions where $P_i''(\chi) > 0$, and

$$U_\chi = -\delta^2\gamma^{-1}P_i''(\chi)\int_0^t T_0(t)\,\mathrm{d}t < 0.$$

The kinetic term $-(\gamma-1)TU_\chi/V$ now assists the rate of increase of temperature T_t. Relative to a homogeneous explosion, one should then expect an increase in local ignition times depending on the value of $P_i''(\chi)$ initially. The greater the magnitude of $P_i''(\chi)$, the greater the effect.

(*b*) *Numerical computation of the evolution from a periodic initial pressure disturbance*

The typical influence of an initial pressure disturbance on the evolution of a reactive atmosphere can be gauged by considering a non-uniform periodic initial disturbance of the form

$$\left.\begin{aligned} P_i(\chi) = 1 + \frac{\nu}{2\beta}\left[\cos\frac{\pi}{\mu}(\chi-\mu)+1\right], \quad T_i(\chi)=1, \quad y_i(\chi)=1, \\ U_i(\chi)=0 \quad \text{and} \quad V_i(\chi)=1/P_i(\chi) \quad \text{for} \quad 0\leqslant\chi\leqslant\mu. \end{aligned}\right\} \tag{6.7}$$

The initial pressure non-uniformity has amplitude ν/β and half-wavelength μ. The temperature, reactant mass fraction and fluid velocity are all assumed to be in a state of initial homogeneity. The first and second derivatives of the non-uniformity in χ-space are given respectively by the values

$$P_i'(\chi) = -\frac{\pi\nu}{2\mu\beta}\sin\frac{\pi}{\mu}(\chi-\mu) \quad \text{and} \quad P_i''(\chi) = -\frac{\pi^2\nu}{2\mu^2\beta}\cos\frac{\pi}{\mu}(\chi-\mu). \tag{6.8}$$

Consequently for $t>0$, the disturbance will initially act to induce volumetric compression for $0\leqslant\chi\leqslant\mu/2$ where $P_i''(\chi)\geqslant 0$, and local volumetric expansion for $\mu/2\leqslant\chi\leqslant\mu$ where $P_i''(\chi)\leqslant 0$. The maximum initial compression and expansion rates will lie at $\chi=0$ and $\chi=\mu$ respectively where $P_i''(0)=\pi^2\nu/2\mu^2\beta$ and $P_i''(\mu)=-\pi^2\nu/2\mu^2\beta$.

The effects generated by an initial pressure disturbance are qualitatively similar to those generated by an initial velocity disturbance; non-uniform rates of fluid divergence for $t>0$ will induce a non-uniform distribution of chemical reaction rates, as the varying distribution of local kinetic flow energy at each χ contribute to non-uniform rates of increase in temperature.

Figure 6*a*, *b* shows the behaviour of the fluid velocity $U(\chi,t)$ and volume $V(\chi,t)$ respectively for a numerical solution of equations (2.1) subject to the initial disturbance (6.7) during reaction at $\chi=0$ for the parameters $\nu=5$, $\mu=1.5$, $Q=3$, $\gamma=1.4$ and $\beta=10$ at the evolution times shown. The early induction stages of the evolution, where the effects of chemistry are weak, display aspects of the oscillatory non-chemical evolution (2.8). For $t>0.77$, a gas expansion is generated near $\chi=0$, leading to the presence of a density maximum in the interior of the fluid. At $t\approx 0.83$, $y=10^{-2}$ and reaction has occurred at $\chi=0$.

The full evolution profiles of temperature and pressure are shown in figures 7*a* and *b* respectively at the stated times. For $t<0.83$, the temperature peak lies at the point of maximum fluid compression initially induced for $t>0$ by the pressure disturbance (6.7), i.e. at $\chi=0$, where reaction has occurred by $t\approx 0.83$. A reaction wave created as the result of the non-uniform ignition times of neighbouring particles arises for $t>0.83$. Pressure wave steepening in the reaction zone is observed during the period $0.83\leqslant t<0.91$. A weak reaction shock has formed in the interior of the reaction wave by $t=0.91$ where $y\approx 0.64$ and is characterized by the pressure jump $5.2\lesssim P\lesssim 9.5$. For $t>0.91$, the reaction shock is continuously amplified, gradually moving towards the front of the reaction wave. At $t=0.99$, the shock lies at a point of reactant consumption within the wave at which $y\approx 0.9$. The pressure jump at this point is given by $2.2\lesssim P\lesssim 16.2$. The Von-Neumann shock pressure associated with a steady strong detonation wave moving into an undisturbed fluid with $Q=3$, $\gamma=1.4$ and $\beta=10$ is given by $P_N=18.9$. It should be noted that the relatively

PHILOSOPHICAL TRANSACTIONS OF THE ROYAL SOCIETY A MATHEMATICAL, PHYSICAL & ENGINEERING SCIENCES

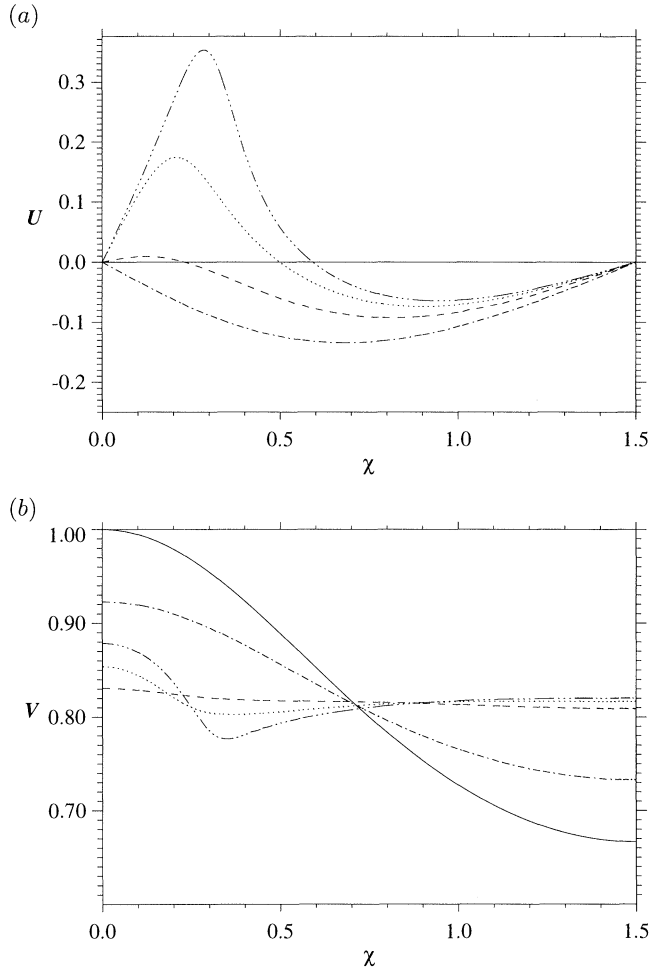

Figure 6. (*a*) The temporal evolution of the fluid velocity $U(\chi, t)$ and (*b*) volume $V(\chi, t)$ during ignition at $\chi = 0$ from the initial disturbance (6.7) for $Q = 3$, $\gamma = 1.4$ and $\beta = 10$ with $\nu = 5$ and $\mu = 1.5$ plotted at the times $t = 0$, (solid line), $t = 0.45$ (dot-dash line), $t = 0.77$ (dashed line), $t = 0.81$ (dotted lines) and $t = 0.83$ (dot-dot-dot-dash line).

high value of the pressure disturbance amplitude $\nu = 5$ required here to permit the initiation of detonation in the system compared with the amplitude of an initial velocity disturbance, corresponds to the relation between the magnitude of the flow divergence rates U_χ required to develop in the fluid in order to generate a sufficient gradient of ignition times and the second derivative of the pressure distribution determined through the relation (6.1).

In figure 8*a* the locus of times where $y = 10^{-2}$ making up the path of the reaction wave calculated numerically from initial conditions (6.7) (solid line) with $\nu = 5$, $\mu = 1.5$, $Q = 3$, $\gamma = 1.4$ and $\beta = 10$ is compared with that obtained from the spontaneous evolution (6.6) (dashed line) with $\delta = 1$. The dotted line represents the uniform path of reaction points obtained when $P_i''(\chi) = 0$ and $y = 10^{-2}$. The spontaneous evolution predicts a reaction time of $t \approx 0.81$ at $\chi = 0$ in comparison with the numerical solution of $t \approx 0.83$. The predictions obtained from the spon-

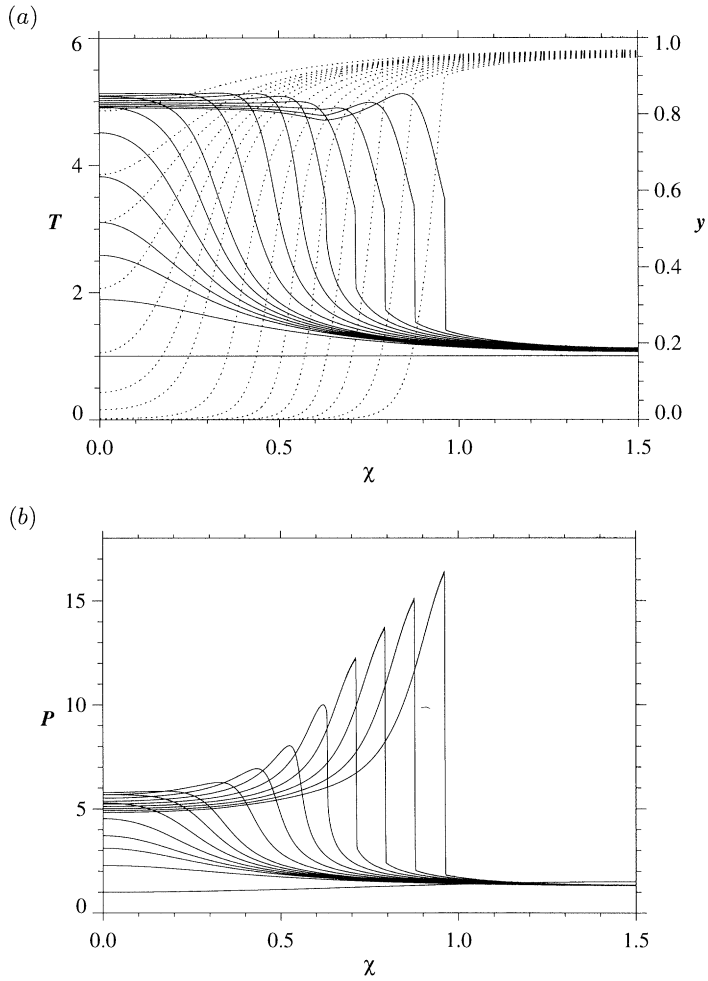

Figure 7. The evolution from initial disturbance (6.7) for $Q = 3$, $\gamma = 1.4$ and $\beta = 10$ with $\nu = 5$ and $\mu = 1.5$ for (a) temperature T (solid lines) and reactant mass fraction y (dotted lines) and (b) pressure P at the times $t = 0$, $t = 0.75$, $t = 0.78$–0.83 (in steps of 1) and $t = 0.85$–0.99 (in steps of 2).

taneous evolution closely follow the numerically calculated solution up to the time $t = 0.91$, when the reaction wave ceases to be shockless. For $P_i''(\chi) > 0$, the spontaneous evolution predicts lower reaction times than the homogeneous reaction time $t_I \approx 1.06$, with the lowest time at $t = 0.81$ at $\chi = 0$. Figure 8b shows the evolution of temperature and reactant mass fraction as predicted by the spontaneous evolution (6.6) with $\delta = 1$ at the times shown. Again, a qualitatively similar evolution to the numerically calculated solution is observed. Therefore up to the point of the reaction shock formation, the spontaneous flame appears to be a reasonable approximation to the numerically calculated solution, whilst being substantially easier to calculate. In addition, it allows for a useful insight into the effects an initial pressure disturbance can have on an evolving atmosphere.

The preceding two sections in which the non-uniform evolution of a reactive system has been initiated from either an initial velocity or pressure disturbance, have

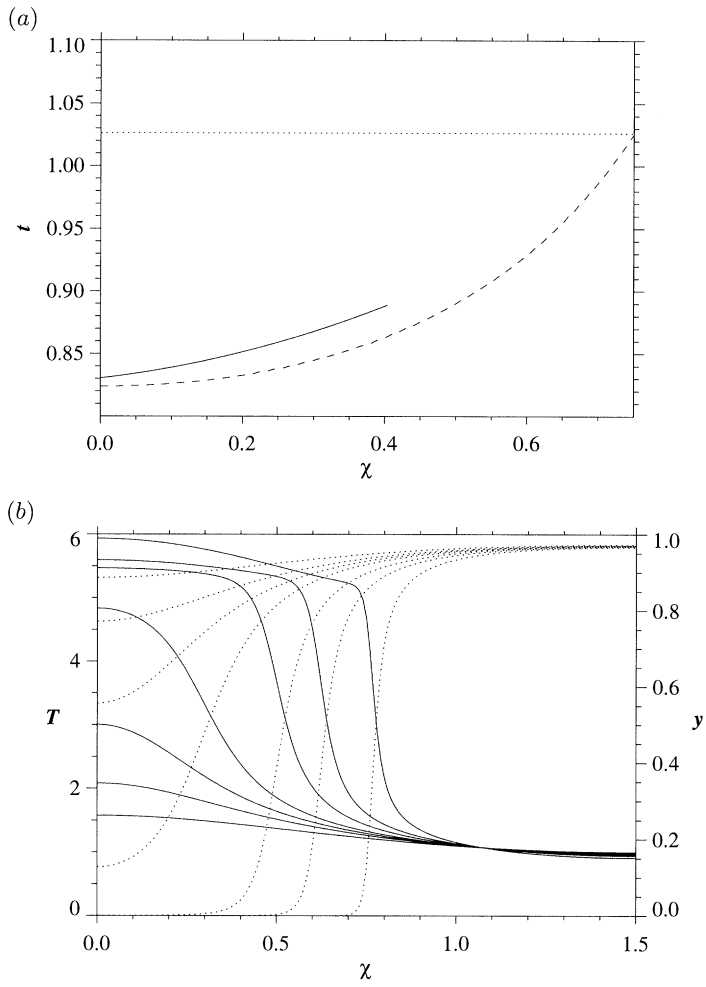

Figure 8. A comparison of the numerically calculated ignition path where $y = 10^{-2}$ (solid line) with the spontaneous path calculated from equations (6.6) (dashed line) and an evolution with $P_i''(\chi) = 0$ (dotted line) and (*b*) the spontaneous evolution of temperature and reactant mass fraction from equations (6.6) shown at the times $t = 0.7$, $t = 0.75$, $t = 0.775$, $t = 0.8$, $t = 0.85$, $t = 0.9$ and $t = 1.0$ for initial conditions (6.7) with $Q = 3$, $\gamma = 1.4$ and $\beta = 10$ with $\nu = 5$ and $\mu = 1.5$.

demonstrated the typical way in which initial gas-dynamic expansion and compression effects can cause non-uniform reaction rates to develop in the system. This leads to the generation of a reaction wave formed due the non-uniform reaction times of neighbouring fluid elements. Since no other heterogeneity is considered in these examples, the gradient of ignition times that lead to detonation is induced by the velocity or pressure disturbance alone; this demonstrates the substantial bearing these non-uniformities can have on the overall evolution of the exothermic system. For general initial conditions involving any combination of both $U = U_i(\chi)$ and $P = P_i(\chi)$, it is expected that a distribution of non-uniform flow divergence rate will be established which serve to act in a similar way to the mechanisms detailed above. In order to usefully appreciate the importance of initial velocity and pressure disturbances in a

reactive fluid, the following two examples discuss the classical evolution from initial temperature or reactant mass fraction non-uniformities in which changes in pressure and velocity occur as the fluid response to the evolution of chemistry.

7. The evolution from an initial temperature disturbance

(a) *The spontaneous flame*

Zeldovich (1980) proposed that the evolution resulting from an initial perturbation in temperature to an otherwise homogeneous atmosphere, such as that investigated by Zeldovich *et al.* (1970), could be estimated by assuming that each particle evolves locally as a uniform constant volume explosion appropriate to its initial state. On this basis, the evolution generated by the initial temperature disturbance

$$T = T_i(\chi), \quad P_i(\chi) = y_i(\chi) = 1, \quad U = U_i(\chi) = 0 \quad \text{and} \quad V = V_i(\chi) = T_i(\chi) \tag{7.1}$$

is obtained from equations (2.1) by setting $U_\chi = P_\chi = 0$ with initial conditions (7.1). The fluid velocity and volume are then respectively determined by the expressions

$$U = 0 \quad \text{and} \quad V = V_i(\chi) = T_i(\chi). \tag{7.2}$$

The temperature is found from the evolution equation,

$$T_t = -\gamma Q y_t \Rightarrow T = T_i(\chi) + \gamma Q(1 - y) \tag{7.3}$$

so that the burnt temperature is given by $T_b(\chi) = T_i(\chi) + \gamma Q$, which decreases with decreasing $T_i(\chi)$. The pressure is given by $P = T/V$ and the reactant mass fraction by

$$-Qy_t = \frac{y}{\beta} \exp\left(\beta\left(1 - \frac{1}{T}\right)\right). \tag{7.4}$$

Combining equation (7.3) and (7.4), the temperature evolution at a given value of χ can be determined by the integral relation,

$$t = \frac{1}{\gamma} \int_{T_i(\chi)}^{T} \frac{1}{\beta^{-1}\left[1 - (T - T_i(\chi))/\gamma Q\right] \mathrm{e}^{\beta(1-1/T)}} \, \mathrm{d}T. \tag{7.5}$$

Equation (7.4) illustrates that non-uniform reaction rates will be immediately established in the fluid due to the initial variation in $T_i(\chi)$. However, it is clearly seen that the spontaneous evolution (7.2)–(7.5) is simply the leading order solution (4.5) which arises for sufficiently slowly varying initial disturbances as formulated in § 4 and thus provides a formal justification for Zeldovich's *ad hoc* formulation.

(b) *Numerical computation of the evolution from an initial periodic temperature disturbance*

The typical influence of an initial temperature disturbance can be ascertained by considering a periodic initial disturbance of the form

$$\left.\begin{aligned} T_i(\chi) = 1 + \frac{\nu}{2\beta}\left[\cos\left(\frac{\pi\chi}{\mu}\right) - 1\right], \quad P_i(\chi) = y_i(\chi) = 1, \\ U_i(\chi) = 0 \quad \text{and} \quad V_i(\chi) = T_i(\chi) \quad \text{for} \quad 0 \leqslant \chi \leqslant \mu \end{aligned}\right\} \tag{7.6}$$

with temperature disturbance amplitude ν/β and half-wavelength μ. The pressure, reactant mass fraction and velocity are all considered to be in a state of initial

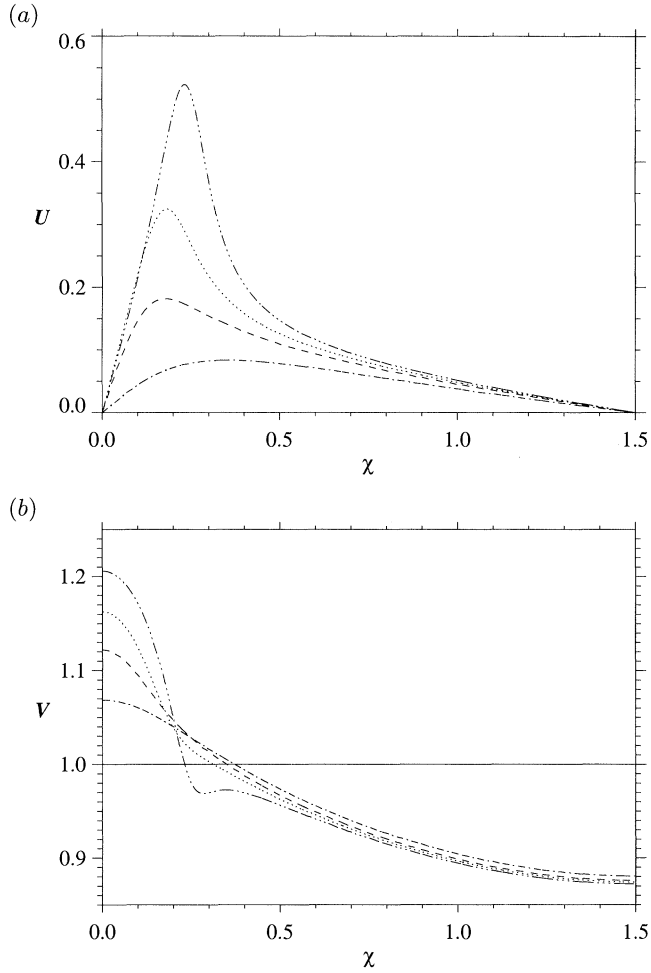

Figure 9. (*a*) The temporal evolution of the fluid velocity $U(\chi, t)$ and (*b*) volume $V(\chi, t)$ from the initial disturbance (7.6) for $Q = 3$, $\gamma = 1.4$ and $\beta = 10$ with $\nu = 1$ and $\mu = 1.5$ plotted at the times $t = 0$, (solid line), $t = 0.96$ (dot-dash line), $t = 1.02$ (dashed line), $t = 1.04$ (dotted line) and $t = 1.06$ (dot-dot-dot-dash line).

homogeneity, while the fluid volume disturbance is identical to the temperature non-uniformity to preserve the gas state relation. The temperature disturbance has gradient

$$T_i'(\chi) = -\frac{\pi\nu}{2\mu\beta} \sin\left(\frac{\pi\chi}{\mu}\right). \tag{7.7}$$

In a non-reactive system, the initial state (7.6) is an equilibrium state, i.e. the system will not evolve unless perturbed by an external force such as chemistry.

For a reaction starting from initial conditions (7.6), varying rates of reactant consumption will immediately be established in the fluid. At $t = 0$, the rate of reactant consumption $-y_t(\chi, 0) = (Q\beta)^{-1} \exp(\beta(1 - 1/T_i(\chi)))$ decreases monotonically from a maximum possible value $1/Q\beta$ at $\chi = 0$ to a minimum value $(1/Q\beta)\exp(-\nu/(1 - \nu/\beta))$ at $\chi = \mu$ ($\nu < \beta$). Figure 9*a*, *b* shows the behaviour of the fluid velocity $U(\chi, t)$ and volume $V(\chi, t)$ respectively for a numerical solution of equations (2.1) with ini-

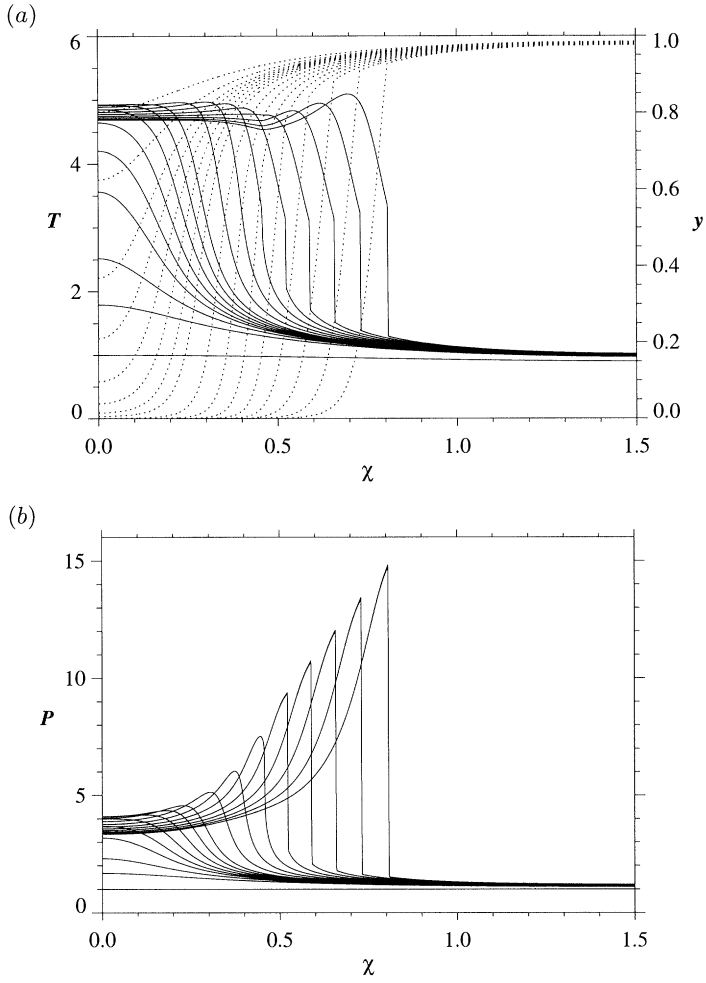

Figure 10. The evolution from initial disturbance (7.6) for $Q = 3$, $\gamma = 1.4$ and $\beta = 10$ with $\nu = 1$ and $\mu = 1.5$ for (a) temperature T (solid lines) and reactant mass fraction y (dotted lines) and (b) pressure P at the times $t = 0$, $t = 0.96$, $t = 1.0$, $t = 1.02$–1.07 (in steps of 1) and $t = 1.09$–1.23 (in steps of 2).

tial conditions (7.6) at the evolution times shown for $\nu = 1$, $\mu = 1.5$, $Q = 3$, $\gamma = 1.4$ and $\beta = 10$. The change in U and V observed here is the dynamic response of the fluid to the non-uniform rate of chemical energy release. A relative expansion of material is generated near $\chi = 0$, associated with the maximum rise in temperature at $\chi = 0$. Reaction has occurred at $\chi = 0$ where $y = 10^{-2}$ in a time $t \approx 1.06$, which is close to the homogeneous reaction time $t \approx 1.02$ when $T_i(\chi) = 1$.

Figure 10a, b shows the evolution of temperature and pressure at the times indicated. The maximum rise in temperature and pressure occurs at $\chi = 0$, until reaction has occurred at $t \approx 1.06$. For $t > 1.06$ a reaction wave moves away from $\chi = 0$, due to the progressive delay in ignition times of particles due to their progressively lower initial temperature. As the reaction wave moves forward, the gradient of the temperature and pressure variation through the reaction zone steepens. At the time $t = 1.15$ a weak reaction shock has developed in the reaction zone, where $y \approx 0.73$ and has a

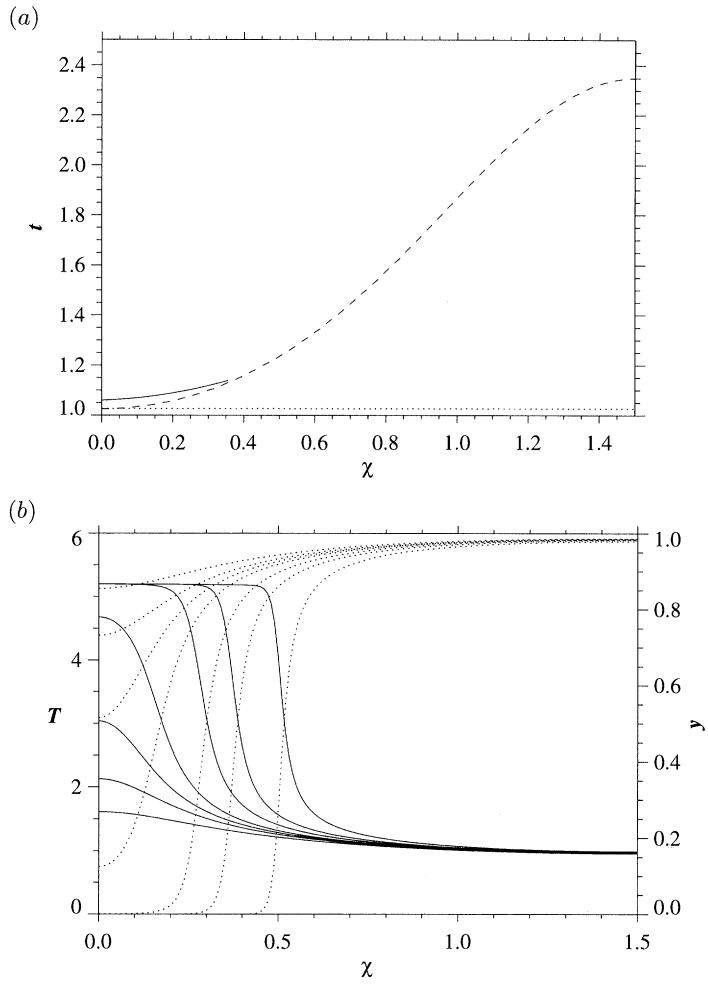

Figure 11. (*a*) A comparison of the numerically calculated ignition path where $y = 10^{-2}$ (solid line) with the constant volume ignition path calculated from equations (7.5) (dashed line) and an evolution with $T_i(\chi) = 1$ (dotted line) and (*b*) the evolution of temperature and reactant mass fraction at constant volume shown at the times $t = 0.9$, $t = 0.95$, $t = 0.975$, $t = 1$, $t = 1.05$, $t = 1.1$ and $t = 1.2$ for initial conditions (7.6) with $Q = 3$, $\gamma = 1.4$ and $\beta = 10$ with $\nu = 1$ and $\mu = 1.5$.

thermodynamic strength determined by the internal pressure jump $2.8 \lesssim P \lesssim 9.5$. For $t > 1.15$, the reaction shock is amplified on moving forward to the head of the reaction zone. At $t = 1.23$ the reaction shock is characterized by the pressure jump $1.5 \lesssim P \lesssim 14.5$.

In figure 11*a* the locus of times where $y = 10^{-2}$ making up the path of the reaction wave calculated numerically from initial conditions (7.6) (solid line) with $\nu = 1$, $\mu = 1.5$, $Q = 3$, $\gamma = 1.4$ and $\beta = 10$ is compared with that obtained from the spontaneous evolution (7.5) (dashed line). The dotted line represents the uniform path of reaction points obtained when $T_i(\chi) = 1$ and $y = 10^{-2}$. The spontaneous evolution predicts a reaction time of $t = 1.02$, in comparison with the numerical solution of $t \approx 1.06$. Figure 11*b* shows the evolution of temperature and reactant mass fraction as predicted by the spontaneous evolution (7.5) at the times shown.

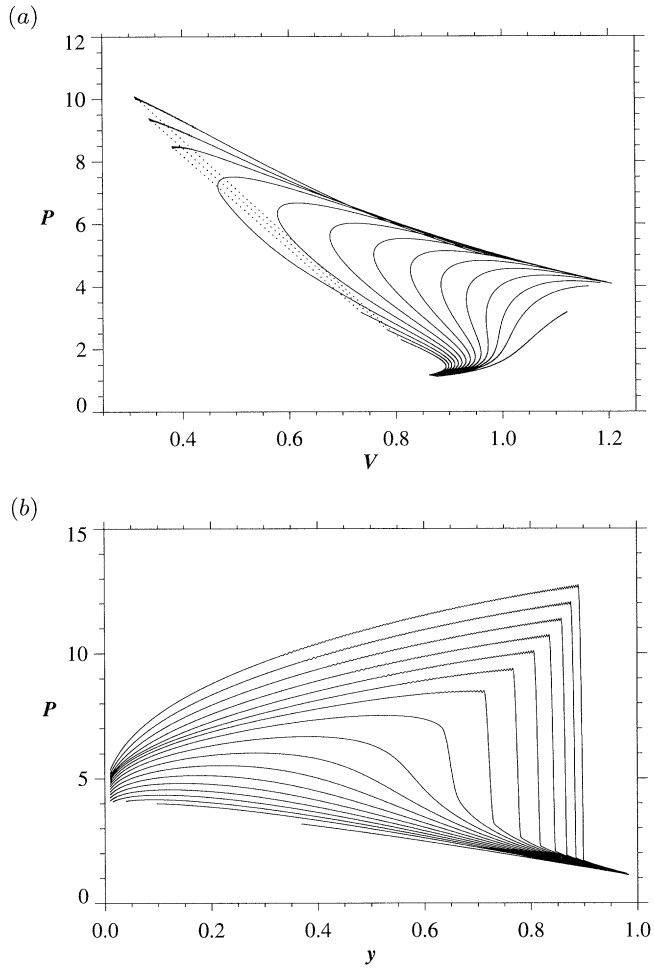

Figure 12. (a) Pressure-volume variation at $t = 1.02$ and $t = 1.04$–1.16 (in steps of 1) and (b) pressure-reactant mass fraction variation at $t = 1.04$–1.20 (in steps of 1) for the initial disturbance (7.6) for $Q = 3$, $\gamma = 1.4$ and $\beta = 10$ with $\nu = 1$, $\mu = 1.5$ and $1 \geqslant y(\chi, t) \geqslant 10^{-2}$ for $t = 1.02$ and $t = 1.04$–1.16 (in steps of 1).

Figures 12a and b respectively show the pressure-volume ($P - V$) variation and pressure-reactant mass fraction variation ($P - y$) for $y \geqslant 10^{-2}$ which arise for $Q = 3$, $\gamma = 1.4$ and $\beta = 10$ from the initial temperature disturbance (7.6) with $\nu = 1$ and $\mu = 1.5$ at the evolution times shown. For reaction from the initial conditions (7.6) a reaction shock has formed by $t = 1.15$ where $y \approx 0.73$. Thus the reaction shock has formed nearer to the front of the reaction wave structure than that observed in figure 5a, b. Qualitatively, however, the unsteady evolution to a strong detonation is similar to that observed in figure 5a, b. One important difference arises in figure 12a, where the initial temperature disturbance creates an initial reaction wave behaviour where the fluid volume increases with increasing pressure. This leads to reaction wave solutions which occur in classically forbidden P–V regions for a steady wave analysis (Fickett & Davies 1979). As reaction further proceeds in the system, the formation of the weak detonation structure (where V decreases with increasing P) within the

flame must then attach to the early expansion behaviour, thereby necessitating the existence of an unsteady transition zone. The existence of reaction wave solutions in this regime again serves to emphasize the unsteadiness of the problem, where the use of a moderate activation energy allows significant expansion effects to occur during reaction.

8. The evolution from an initial reactant mass fraction non-uniformity

(*a*) *The spontaneous flame*

The leading order spontaneous evolution arising from an initial reactant concentration disturbance of the form

$$y = y_i(\chi), \quad T_i(\chi) = P_i(\chi) = 1, \quad U = U_i(\chi) = 0, \quad \text{and} \quad V_i(\chi) = 1 \tag{8.1}$$

is obtained in a similar way as that for an initial temperature disturbance, i.e. by setting $\delta = 0$ in equations (2.1). It follows (§ 4) that the fluid velocity and volume are determined by,

$$U = 0 \quad \text{and} \quad V = 1, \tag{8.2}$$

the temperature by

$$T_t = -\gamma Q y_t \Rightarrow T = 1 + \gamma Q(y_i(\chi) - y), \tag{8.3}$$

the pressure by $P = T/V$ and reactant mass fraction by

$$-Qy_t = \frac{y}{\beta} \exp\left(\beta\left(1 - \frac{1}{T}\right)\right). \tag{8.4}$$

Equations (8.3) and (8.4) can now be combined with conditions (8.1) to give

$$t = \frac{1}{\gamma}\int_1^T \frac{1}{\beta^{-1}\left[y_i(\chi) - (T-1)/\gamma Q\right] \mathrm{e}^{\beta(1-1/T)}}\,\mathrm{d}T. \tag{8.5}$$

The burnt temperature $T_\mathrm{b}(\chi) = 1 + \gamma Q y_i(\chi)$ decreases with a decrease in $y_i(\chi)$. By differentiating the integral expression (8.5) with χ, it can be shown that in order to generate an $O(1)$ gradient in reaction times, an initial disturbance in reactant mass fraction must be taken such that its gradient has an order one variation in space. This compares with disturbance gradients of $O(\beta^{-1})$ required by non-uniformities in velocity, pressure or temperature to achieve the same effect.

(*b*) *Numerical computation of the evolution from an initial periodic reactant mass disturbance*

The primary effects of an initial reactant mass fraction disturbance on the generation of a reaction wave can be ascertained by considering a periodic initial disturbance of the form

$$y_i(\chi) = \exp[\tfrac{1}{2}\nu(\cos(\pi\chi/\mu) - 1)], \quad P_i(\chi) = T_i(\chi) = V_i(\chi) = 1 \quad \text{and} \quad U_i(\chi) = 0, \tag{8.6}$$

such that the disturbance has amplitude $\mathrm{e}^{-\nu}$, half-wavelength μ and disturbance gradient

$$y_i'(\chi) = -\frac{\pi\nu}{2\mu}\sin\left(\frac{\pi\chi}{\mu}\right)\exp[\tfrac{1}{2}\nu(\cos(\pi\chi/\mu) - 1)] \quad \text{for} \quad 0 \leqslant \chi \leqslant \mu, \tag{8.7}$$

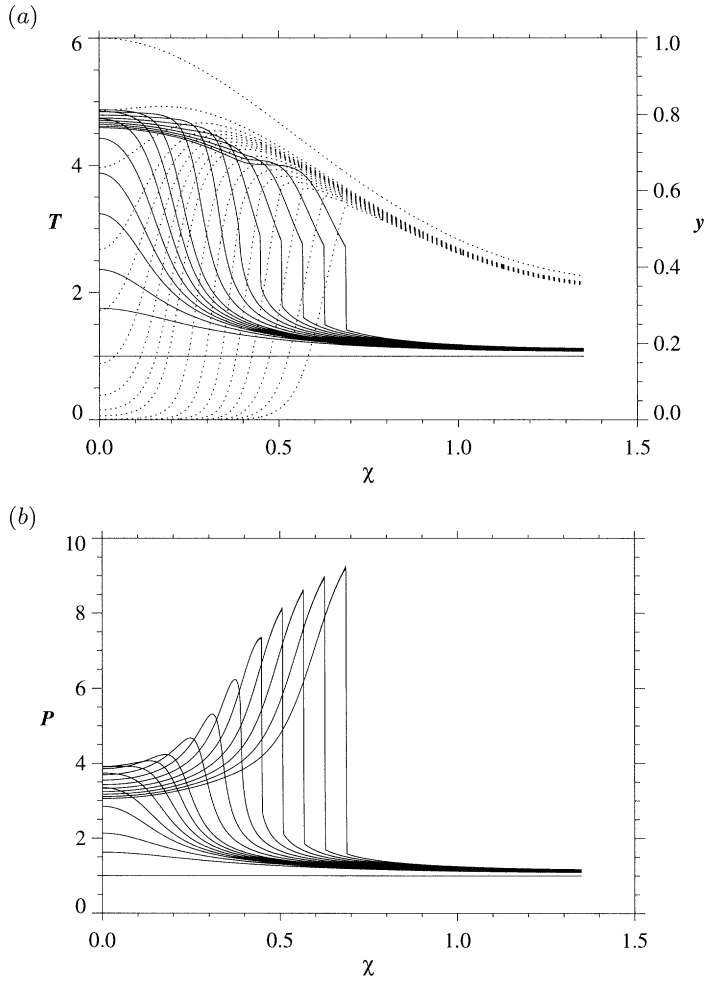

Figure 13. The evolution from initial disturbance (8.6) for $Q = 3$, $\gamma = 1.4$ and $\beta = 10$ with $\nu = 1$ and $\mu = 1.5$ for (a) temperature T (solid lines) and reactant mass fraction y (dotted lines) and (b) pressure P at the times $t = 0$, $t = 0.96$, $t = 1.0$, $t = 1.02$–1.07 (in steps of 1) and $t = 1.09$–1.23 (in steps of 2).

with $y_i(0) = 1$, $y_i(\mu) = \mathrm{e}^{-\nu}$. The fluid temperature, pressure, volume and velocity are all assumed to be in an initial state of homogeneity. Since $P_i'(\chi) = 0$ and $U_i'(\chi) = 0$, the initial rate of increase of temperature, pressure and reactant mass fraction is determined by the relations $T_t = P_t = \gamma y_i(\chi)/\beta$ and $y_t = -y_i(\chi)/Q\beta$ respectively. Thus, the rate of temperature change decreases monotonically from a maximum possible value γ/β at $\chi = 0$ to a minimum value $\gamma \mathrm{e}^{-\nu}/\beta$ at $\chi = \mu$. After a small time step Δt into the evolution, the gas state is then determined as $V(\chi, \Delta t) = 1$, $U(\chi, \Delta t) = 0$, $T(\chi, \Delta t) = P(\chi, \Delta t) = 1 + \gamma y_i(\chi)\Delta t/\beta$ and $y(\chi, \Delta t) = 1 - y_i(\chi)\Delta t/Q\beta$, as $\Delta t \to 0$. A non-uniform rate of increase in velocity is established at Δt, where $U_t(\chi, \Delta t) = -\gamma^{-1} P_\chi(\chi, \Delta t) = -y_i'(\chi)\Delta t/\beta > 0$, so that $U_t(\chi, \Delta t)$ has a positive maximum value at $\chi = \mu/2$.

The situation of an initial reactant mass fraction non-uniformity is of special interest with regard to both the generation of a non-uniform locus of ignition times

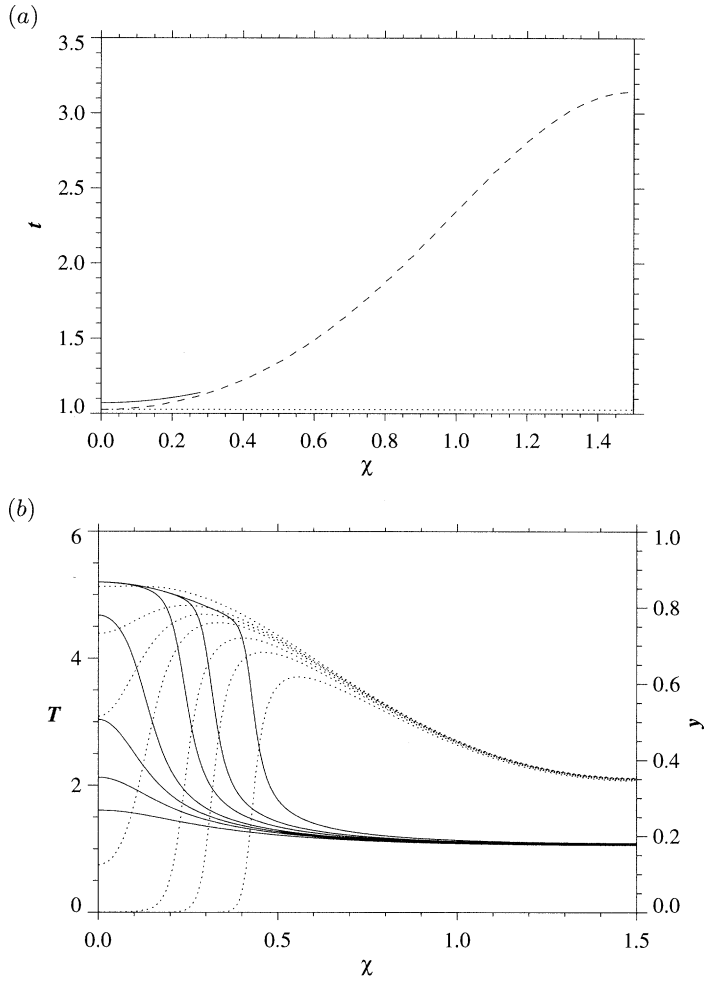

Figure 14. (*a*) A comparison of the numerically calculated ignition path where $y(\chi) = 10^{-2} y_i(\chi)$ (solid line) with the fixed volume ignition path calculated from (8.5) (dashed line) and an evolution with $y_i(\chi) = 1$ (dotted line) and (*b*) the evolution of temperature and reactant mass fraction with fixed volume shown at the times $t = 0.9$, $t = 0.95$, $t = 0.975$, $t = 1$, $t = 1.05$, $t = 1.1$ and $t = 1.2$ for initial conditions (8.6) with $Q = 3$, $\gamma = 1.4$ and $\beta = 10$ with $\nu = 1$ and $\mu = 1.5$.

and the evolution of the reaction shock. Figure 13*a*, *b* shows the evolution of temperature and pressure with χ for reaction from initial conditions (8.6) at the stated times for the case $Q = 3$, $\gamma = 1.4$, $\beta = 10$, $\nu = 1$ and $\mu = 1.5$. Reaction has occurred at $\chi = 0$ at $t \approx 1.06$. A reaction shock is observed to form at $t = 1.15$. However, unlike the previous examples, the reaction shock is only weakly amplified on moving through the flame structure and the evolved planar strong detonation at $t = 1.23$ has a maximum pressure less than twice the Von-Neumann pressure associated with a Chapman–Jouguet detonation moving into a homogeneous medium with $y_i(\chi) = 1$. Due to the decrease in initial concentration of reactant, there is a loss of potential chemical energy off which the shock can amplify and the growth of the reaction shock is restricted during its propagation through the reaction zone.

In figure 14*a* the locus of reaction times making up the path of the flame, where $y = 10^{-2}$ at each χ, calculated numerically from initial conditions (8.6) (solid line) with $\nu = 1$, $\mu = 1.5$, $Q = 3$, $\gamma = 1.4$ and $\beta = 10$ is compared with that obtained from the spontaneous evolution (8.5) (dashed line). The dotted line represents the uniform path of reaction points obtained when $y_i(\chi) = 1$ and $y = 10^{-2}$. Figure 14*b* shows the evolution of temperature and reactant mass fraction as predicted by the spontaneous evolution (8.2)–(8.5) at the times shown. Again, a close resemblance to the numerically calculated solution is observed.

9. Summary

The important role played by initial velocity and pressure disturbances in a combustible gas reacting exothermically from initial non-uniformities has been demonstrated. Such initial disturbances generate non-uniform local fluid divergence rates, which in turn lead to a non-uniform gradient of ignition times in the material similar to the previously known effect created by initial non-uniform temperature or reactant mass concentration disturbances. If the amplitudes of the initial velocity or pressure disturbances are sufficiently large, these non-uniformities can be the sole cause of the creation of a strong detonation in the system. In the general situation, where the distributions $U_i'(\chi)$, $P_i'(\chi)$, $T_i'(\chi)$ and $y_i'(\chi)$ are all non-zero at the initial time, each disturbance will act to generate particular reaction rate non-uniformities which in combination determine the eventual locus of ignition points. An asymptotic formulation of the spontaneous flame concept due to Zeldovich (1980) arising from general initial non-uniform disturbances has been constructed on the basis of slowly varying initial disturbances. The leading order terms in this expansion correspond to Zeldovich's formulation, but are shown only to capture the effects of initial temperature and concentration non-uniformities. Lower order corrections include the effects of initial velocity and pressure disturbances.

The reaction wave structure arising from reaction at initial conditions has also been investigated. A similarity between the present flame structures and those of Singh & Clarke (1992) has been found. This suggests that the use of realistic moderate activation energies can result in unsteady reaction structures, where compressibility effects are able to propagate during the stages of significant chemical reaction. In such cases quasi-steady reaction wave approximations (Dold & Kapila 1995*b*) appropriate for large activation energies do not provide a good representation of the reaction wave structure.

The author thanks both Professor J. F. Clarke, F.R.S., and Dr J. W. Dold for valuable discussions associated with the present work.

References

Almgren, R. 1992 High-frequency acoustic waves in a reacting gas *SIAM J. Appl. Math.* **51**, 351–373.

Blythe, P. A. 1978 Wave propagation and ignition in a combustible mixture. In *Proc. 17th Symp. (Int.) on Combustion*, pp. 909–916.

Clarke, J. F. 1979 On the evolution of compression pulses in an exploding atmosphere; initial behaviour. *J. Fluid Mech.* **94**, 195–208.

Bdzil, J. B. & Kapila, A. K. 1992 Shock-to-detonation transition. *Phys. Fluids* A **4**, 409–418.

PHILOSOPHICAL TRANSACTIONS OF THE ROYAL SOCIETY A MATHEMATICAL, PHYSICAL & ENGINEERING SCIENCES

Dold, J. W. & Kapila, A. K. 1995*a* Asymptotic analysis of detonation initiation for one-step chemistry. 1. Emergence of a weak detonation. (In preparation.)

Dold, J. W. & Kapila, A. K. 1995*b* Asymptotic analysis of detonation initiation for one-step chemistry. 2. From a weak structure to ZND. (In preparation.)

Dold, J. W., Clarke, J. F. & Short, M. 1995 Steady and unsteady aspects of detonation initiation. (In the press.)

Fickett, W. & Davies, W. C. 1979 *Detonation.* Berkeley: University of California Press.

Gel'fand, B. E., Polenov, A. N., Frolov, S. M. & Tsyganov, S. A. 1985 On the onset of detonation in a non-uniformly heated gas mixture. *Fizika Goreniya Vzryva* **21**, 118–123.

Kassoy, D. R. 1975 A theory of adiabatic, homogeneous explosion from initiation to completion. *Combust. Sci. Tech.* **10**, 27–35.

Kassoy, D. R. & Clarke, J. F. 1985 The structure of a high speed deflagration with a finite origin. *J. Fluid Mech.* **150**, 253–280.

Majda, A. J. & Rosales, R. 1987 Nonlinear mean-field-high-frequency wave interactions in the induction zone. *SIAM J. Appl. Math.* **47**, 1017–1039.

Stewart, D. S. 1986 Plane shock initiation of homogeneous and heterogeneous condensed phase explosives with a sensitive rate. *Combust. Sci. Tech.* **48**, 205–262.

Stewart, D. S. 1988 Shock induced thermal explosion. *Mathematical modelling of combustion and related topics*, pp. 301–314. Martinus Nijhoff.

Singh, G. & Clarke, J. F. 1992 Transient phenomena in the initiation of a mechanically driven detonation. *Proc. R. Soc. Lond.* A **438**, 23–46.

Zeldovich, Ya. B., Librovich, V. B., Makhviladze, G. M. & Sivashinsky, G. I. 1970 Development of detonation in a non-uniformly preheated gas. *Astr. Acta* **15**, 313–321.

Zeldovich, Ya. B. 1980 Regime classification of an exothermic reaction with non-uniform initial conditions. *Combust. Flame* **39**, 211–214.

Zeldovich, Ya. B., Gelfand, B. E., Tsyganov, S. A., Frolov, S. M. & Polenov, A. N. 1988 Concentration and temperature non-uniformities (CTN) of combustible mixtures as a reason of pressure wave generation. In *Proc 11th Colloquim (Int.) on Dynamics of Explosions and Reactive systems*, pp. 99–123. Warsaw.

Received 25 June 1993; accepted 9 November 1993

PHILOSOPHICAL TRANSACTIONS OF THE ROYAL SOCIETY A MATHEMATICAL, PHYSICAL & ENGINEERING SCIENCES